



TOMÁS ALEXANDRE DIAS PEDREIRA
BSc in Electrical and Computer Engineering

MOTION PLANNING FOR A TRACTOR-TRAILER SYSTEM IN SMART AGRICULTURE

MASTER IN ELECTRICAL AND COMPUTER ENGINEERING
SPECIALIZATION IN ROBOTICS AND CONTROL

NOVA University Lisbon
September, 2025



MOTION PLANNING FOR A TRACTOR-TRAILER SYSTEM IN SMART AGRICULTURE

TOMÁS ALEXANDRE DIAS PEDREIRA

BSc in Electrical and Computer Engineering

Adviser: Ricardo Alexandre Fernandes da Silva Peres

Assistant Professor, NOVA University Lisbon

Co-adviser: Alexandre Miguel Manta da Costa

Research Engineer, NOVA University Lisbon

Examination Committee

Chair: Name of the committee chairperson
Full Professor, FCT-NOVA

Rapporteur: Name of a rapporteur
Associate Professor, Another University

Members: Another member of the committee
Full Professor, Another University
Yet another member of the committee
Assistant Professor, Another University

MASTER IN ELECTRICAL AND COMPUTER ENGINEERING
SPECIALIZATION IN ROBOTICS AND CONTROL

NOVA University Lisbon
September, 2025

MOTION PLANNING FOR A TRACTOR-TRAILER SYSTEM IN SMART AGRICULTURE

Copyright © Tomás Alexandre Dias Pedreira, NOVA School of Science and Technology, NOVA University Lisbon.

The NOVA School of Science and Technology and the NOVA University Lisbon have the right, perpetual and without geographical boundaries, to file and publish this dissertation through printed copies reproduced on paper or on digital form, or by any other means known or that may be invented, and to disseminate through scientific repositories and admit its copying and distribution for non-commercial, educational or research purposes, as long as credit is given to the author and editor.

This document was created with the (pdf/Xe/Lua) \LaTeX processor and the [NOVAtesis](#) template (v7.3.9) [1].

To my grandparents.

”

“Impossible is a word to be found only in the dictionary of fools.”

— **Napoleon Bonaparte**, Somewhere in a book or speech
(French Emperor)

ABSTRACT

Over the years, the world of technology has been expanding in every possible field, and agriculture is no exception. The use of technology in Smart Agriculture has been increasing, with Internet of Things networks, Artificial Intelligence systems for management and forecasting, and robotics to automate processes, performing repetitive jobs humans would rather not do, such as applying pesticides, harvesting products, and evaluating the state of the fields, as well as tasks humans cannot easily accomplish, like surveilling large fields. These developments not only facilitate tasks but also address ongoing challenges in the agricultural sector, including the shortage of young people willing to undertake demanding fieldwork and the growing global population, which will heighten the demand for food production. This task is inherently challenging, and the addition of a trailer to the system increases the complexity, as the trailer's dynamics must be accounted for. The tractor-trailer system was chosen, despite its complexity and limited documentation, due to its modularity, enabling independent operation and reusability. This thesis presents the development of a tractor-trailer robotic system capable of autonomously navigating through a field. It includes a review of robotic applications in Smart Agriculture and an exploration of popular robot path planning methods like the Voronoi Graph, A* grid search along with others. This work also reviews several control methods including Dynamic Window Approach, Pure Pursuit, and Model Predictive Control. The selected methods implemented and tested were the Voronoi Graph combined with the Hybrid A* algorithm for path planning and the Pure Pursuit controller for trajectory tracking. The system was architected with hardware components, custom planner and controller plugins in ROS2 and NAV2 stack and collision detection mechanisms. Tests conducted in simulation and real-world environments evaluated path tracking in direct, obstructed, and recovery scenarios, as well as obstacle detection, demonstrating the system's effectiveness in navigation and safety while highlighting areas for improvement.

Keywords: Smart Agriculture, tractor-trailer, Path planning, Trajectory tracking, Robot control, ROS2, NAV2, Voronoi Graph, Hybrid A*, Pure Pursuit

RESUMO

Ao longo dos anos, a tecnologia tem-se expandido em todos os campos, e a agricultura não é exceção. A utilização na Agricultura Inteligente tem aumentado, com redes de Internet das Coisas, sistemas de Inteligência Artificial para gestão e previsão, e robótica para automatizar processos, realizando tarefas repetitivas que humanos preferem evitar, como aplicar pesticidas, colher produtos e avaliar campos, além de tarefas difíceis como vigiar grandes áreas. Estes desenvolvimentos facilitam tarefas e abordam desafios no setor agrícola, como a escassez de jovens para trabalhos de campo exigentes e o crescimento da população global, intensificando a demanda por alimentos. Esta tarefa é desafiante, e a adição de um atrelado aumenta a complexidade, pois as dinâmicas do atrelado devem ser consideradas. O sistema tractor-trailer foi escolhido, apesar da complexidade e documentação limitada, pela sua modularidade, permitindo operação independente e reutilização. Esta tese apresenta o desenvolvimento de um sistema robótico tractor-trailer capaz de navegar autonomamente num campo. Inclui revisão de aplicações robóticas na Agricultura Inteligente e exploração de métodos de planeamento de trajetórias para robôs, como o Voronoi Graph, A* juntamente com outros. Revê também métodos de controlo, incluindo Dynamic Window Approach, Pure Pursuit e Model Predictive Control. Os métodos selecionados, implementados e testados, foram o Voronoi Graph combinado com Hybrid A* para planeamento de trajetórias e Pure Pursuit para seguimento de trajetória. O sistema foi arquitetado com plugins personalizados de planeador e controlador na stack ROS2 e NAV2, e mecanismos de deteção de colisões. Testes em simulação e no mundo real avaliaram o seguimento de trajetórias em cenários diretos, obstruídos e de recuperação, além da deteção de obstáculos, demonstrando eficácia na navegação e segurança, destacando áreas para melhoria.

Palavras-chave: Agricultura Inteligente, tractor-trailer, Planeamento de trajetórias, Seguimento de trajetória, Controlo, ROS2, NAV2, Voronoi Graph, Hybrid A*, Pure Pursuit

CONTENTS

Contents	vi
List of Figures	ix
List of Algorithms	xii
Acronyms	xiii
1 Introduction	1
1.1 Background	1
1.2 Motivation	1
1.3 Document Structure	2
2 Literature Review	3
2.1 Mobile Robotics in Smart Agriculture	3
2.2 Motion Planning	5
2.2.1 Cell Decomposition approaches	6
2.2.2 Grid/Graph Search algorithms	7
2.2.3 Artificial Potential Field	9
2.2.4 Sampling-based approaches	10
2.2.5 Roadmapping approaches	11
2.2.6 Bio-Inspired approaches	12
2.2.7 Learning-based approaches	15
2.3 Motion Control	16
2.3.1 Pure Pursuit	16
2.3.2 Model Predictive Controller	17
2.3.3 Dynamic Window Approach	17
2.4 Localization and Mapping	17
2.4.1 Localization	18
2.4.2 Mapping	18

2.5	Related Work	18
2.5.1	System Description	18
2.5.2	Applications	19
2.6	State of the art Summary	22
3	Architecture	23
3.1	System Overview	23
3.2	Planner	24
3.3	Controller	28
3.4	Collision Avoidance	29
3.5	Final Architecture	30
4	Implementation	32
4.1	Software	32
4.1.1	ROS2	32
4.1.2	NAV2	33
4.2	Hardware	34
4.3	Environment	36
4.4	Planning algorithm	40
4.4.1	Voronoi Graph	40
4.4.2	Planner Plugin	45
4.5	Controller Plugin	50
4.6	Behaviour Tree	51
5	Tests and Results	52
5.1	Path Tracking Tests	52
5.1.1	Direct Path	53
5.1.2	Obstructed Path	55
5.1.3	Recovery test	57
5.2	Obstacle detection Tests	61
5.2.1	Simulation Results	61
5.2.2	Real World Results	63
5.3	Discussion	63
5.3.1	Path Tracking	63
5.3.2	Obstacle Detection and Safety	65
6	Conclusion and Future Work	66
6.1	Conclusion	66
6.2	Future Work	67
Bibliography		68
Annexes		

I Annex 1 Clips **74**

II Annex 2 Code **75**

LIST OF FIGURES

2.1 Exact Cell Decomposition representation; Green line is a possible chosen path.	6
2.2 Adaptive Cell Decomposition representation; Green Squares are the chosen cells/nodes for the shortest path	7
2.3 Approximate 8-connected Cell Decomposition representation; Arrows represent every possible movement the robot can make	7
2.4 (a)	8
2.5 (b)	8
2.6 (c)	8
2.7 8-connected Dijkstra's Algorithm; a) is the starting C-space; b) is a mid point of the algorithm; c) is the end point of the algorithm; The green squares are the searched neighbours, the red ones are the visited nodes and the blue ones are the chosen path.	8
2.8 (a)	9
2.9 (b)	9
2.10 (c)	9
2.11 8-connected A* Algorithm; a) is the starting C-space; b) is a mid point of the algorithm; c) is the end point of the algorithm; The green squares are the searched neighbours, the red ones are the visited nodes and the blue ones are the chosen path.	9
2.12 APP algorithm; On the left is the normal functioning of the algorithm where the pink arrows represent obstacle repulsion, the smaller blue ones represent the goal attraction and the curvy blue arrow is the chosen path; On the right is the local minima situation.	9
2.13 Visibility Graph representation; As explained, the black lines are the connections between the vertices that will then be searched for the shortest path . . .	12
2.14 Voronoi Diagram representation; The black lines keep the same distance to the obstacles and the map edges	13
3.1 Planner logic flowchart	25
3.2 Hybrid A* node expansion.	28

3.3	Representation of the collision detection module. In red the goal pose, in grey the tractor, the black circle is the obstacle and then the dotted rectangle the expanded rectangle used to check for collisions.	30
3.4	System architecture overview. In pink are the components that have been implemented or configured, and in green the already available components.	31
4.1	NAV2 stack architecture [49]	33
4.2	Simulated tractor in Gazebo.	34
4.3	Real tractor.	35
4.4	Agilex Scout dimensions [50].	35
4.5	Tractor-trailer system simulated in Gazebo Classic.	36
4.7	Map created using the SLAM Package in the Gazebo Simulation. White space is non-occupied space, black are obstacles and grey is undiscovered space. .	37
4.6	Gazebo world used for simulation.	37
4.8	Map of the concealed room.	38
4.9	Map of the corridor.	39
4.10	Rviz2 visualization of the robot in the simulated environment.	40
4.11	Image with the obstacle edges.	41
4.12	First Voronoi Graph created for the environment in figure 4.6.	41
4.13	Second Voronoi Graph created for the environment in figure 4.6.	42
4.14	Final Voronoi Graph created for the environment in figure 4.6.	42
4.15	Concealed room Graph.	43
4.16	Corridor Graph.	44
4.17	Subpath, in blue, created by the planner.	45
4.18	Dubins Path created by the planner in the first iteration.	46
4.19	Dubins Path created by the planner in three tries. The red circle marks the subgoal used as intermediary.	47
4.20	Hybrid A* arcs.	48
4.21	Successful recovery path with number of segments as one. Hybrid A* path in red, Dubins path in green, and subgoals in blue.	48
4.22	Successful recovery path with number of segments as fifteen. Hybrid A* path in red, Dubins path in green, and subgoals in blue.	49
4.23	Trailer's positions in pink. Tractor's positions in green.	50
5.1	Direct path test setup in the simulated environment. Goal pose in yellow. .	53
5.2	Direct path test setup in the corridor. Goal pose in yellow.	54
5.3	Obstructed path test setup in the simulated environment. Goal pose in yellow.	55
5.4	Obstructed path test setup in the corridor. Goal pose in yellow.	56
5.5	Recovery test setup in the simulated environment. Goal pose in yellow. . .	57
5.6	Recovery test setup in the real world environment. Goal pose in yellow. . .	58

5.7	Test where the resulting path was slightly different from the originally planned one.	59
5.8	Test where the path had too many manoeuvres for the controller to handle.	60
5.9	Recovery correction of the previous test setup in the real world environment.	60
5.10	Initial configuration in the simulated environment.	61
5.11	Initial path in the simulated environment. The blue arrows coming out from the tractor represent the collision detection range.	62
5.12	Final configuration in the simulated environment. The cylinder was moved and the robot stopped in the parameterised range.	62
5.13	Failed attempt where the robot needed to invert its pose within the corridor, leading to multiple successive changes in directions. Video also annexed.	64

LIST OF ALGORITHMS

1	Planner Pseudocode	26
2	Get_subgoals Pseudocode	27
3	Expand_hybrid_node Pseudocode	28

ACRONYMS

ACO	Ant Colony Optimization (<i>pp. 12, 14</i>)
AMCL	Adaptive Monte Carlo Localization (<i>p. 18</i>)
APF	Artificial Potential Field (<i>pp. 9, 10, 13, 21</i>)
DWA	Dynamic Windows Approach (<i>pp. 16, 17</i>)
FAO	Food and Agriculture Organization (<i>p. 1</i>)
GA	Genetic Algorithm (<i>pp. 13, 15</i>)
MIARs	Multi-functional Intelligent Agricultural Robots (<i>p. 4</i>)
MPC	Model Predictive Controller (<i>pp. 16, 17, 21, 22, 67</i>)
NAV2	Navigation 2 (<i>pp. 33, 37, 45, 50, 65, 66</i>)
PP	Pure Pursuit Controller (<i>pp. 16, 17, 21, 22, 28</i>)
PRM	Probabilistic Roadmap (<i>pp. 10, 11</i>)
PSO	Particle Swarm Optimization (<i>pp. 12–14</i>)
ROS	Robot Operating System (<i>p. 32</i>)
ROS2	Robot Operating System 2 (<i>pp. 32, 33, 36, 38, 40, 66</i>)
RRT	Rapidly-exploring Random Tree (<i>pp. 10, 11</i>)
SLAM	Simultaneous Localization and Mapping (<i>pp. 18, 37, 38</i>)
SVM	Support Vector Machines (<i>p. 15</i>)
UAV	Unmanned Aerial Vehicle (<i>pp. 3, 4, 11</i>)
UGV	Unmanned Ground Vehicle (<i>pp. 3, 12</i>)
URDF	Unified Robot Description Format (<i>pp. 46, 75</i>)

INTRODUCTION

In this chapter, there will be a background explanation of the proposed problem, the motivation for a solution and the document structure.

1.1 Background

Agriculture is one of the most essential industries, providing a source of food for the growing population around the globe. However, the industry faces several challenges, such as the need to increase food production, for example, according to the [Food and Agriculture Organization \(FAO\)](#) of the United Nations, around eight hundred million people are undernourished, and two thirds of them live in Asia. For example, in India, over 70% of the population is dependent on agriculture for their livelihood [2], and, due to lack of the development of the countries' agricultural processes, most farmers use very traditional methods of farming, which are not efficient requiring a lot of time and manual labour. To overcome these issues and to meet the growing demand for food, the agriculture industry is turning to technology, such as robotics, to improve efficiency and productivity.

The use of technologies like AI, Internet of Things, and robotics facilitates the automation of several tasks, such as planting, weeding, harvesting, forecasting, and monitoring which tackles the issues of labour shortages and allowing for easier expansion, solving the need for more food production. One particularly important application of robotics in agriculture is in pesticide spraying. Traditionally, pesticide application has been a labour-intensive and slow task. Autonomous pesticide spraying robots address these issues by applying pesticides more accurately, reducing chemical waste, and minimizing human exposure to harmful substances.

1.2 Motivation

The motivation behind the development of a tractor-trailer pesticide spraying robot is the need to improve agricultural processes to meet the demand for food production and

safety. By integrating these robots in Smart Farming, farmers can optimize pesticide usage, reducing the amount of pesticide wasted and overexposure to chemicals. The solution proposed in this work is to develop a trailer-tractor system, where the tractor will be responsible for towing a trailer with a pesticide spraying system. The advantages of this system are its modularity, with each part acting independently, allowing for easier reuse and maintenance, and also the fact that the development of the robot is not constrained by the functionality of the system to be integrated, meaning that the tractor can be developed freely without having to account for the space occupied by the fluid tanks and balancing fluid tanks, leaving more room to develop both systems independently.

The main technical issue with these systems is their non-holonomic characteristics, meaning that the tractor has its movement restricted due to the trailer's dynamics. A good example of a problem these systems can have is when a differential drive robot tries to rotate in place, the trailer will simply be dragged along, drifting sideways, where it might end up in a position that isn't the desired one or even capsizing. This dynamic makes planning and control very challenging since both the planning and control systems will have to account for the constraint on the turning radius of the tractor-trailer system when calculating a path and sending motion commands.

When analysing the advantages and disadvantages of the proposed system, it is clear that, with a good path planning and motion control solution, the advantages far outweigh the disadvantages making the proposed solution a viable approach for increasing safety and efficiency in smart agriculture.

1.3 Document Structure

This document is divided into 6 chapters. The first chapter is the introduction, where the problem is presented along with the motivation for the work and the document structure.

The second is the state of the art review, where a contextualization of mobile robotics in agriculture is made along with the most popular methods for path planning and robot control along with some previous work on the trailer-tractor system.

The third chapter is the architecture of the proposed solution, it exposes how every component of the system works as well as some additional contextual information on the hardware and software used.

The fourth chapter is the implementation, here the implementation of each component explained in the previous chapter is detailed, along with its development along with some challenges faced during the process and how they were overcome.

The fifth chapter presents the tests and results done and obtained at the end of the work, demonstrating the effectiveness and reliability of the proposed solution.

The sixth and last chapter is the conclusion and future work, where a summary of the document is presented along with some suggestions for future research directions.

LITERATURE REVIEW

In this chapter, four main topics will be explored: Mobile Robotics in Smart Agriculture, Motion Planning and its Approaches, Robot Control Methods, and Tractor-Trailer-like System Applications, as well as an analysis of the results.

2.1 Mobile Robotics in Smart Agriculture

According to UNESCO, the world population is going to increase by about 30% in the next 25 years and with it, the need for food production. To satisfy this need, there will have to be an upgrade in agricultural production and to do it, there has been a development of IoT and AI technologies to help gather information and make better decisions about the crop fields [3]. These technologies acquire data using several sensors, such as humidity sensors, pH sensors, temperature sensors and substance level sensors, that communicate wirelessly using a variety of case dependent protocols (like ZigBee or LoRa) to make decisions using specific algorithms like PID controllers, Time-Controlled algorithms, Fuzzy-Logic or Machine Learning algorithms like neural networks.

According to [4, 5] there are also other factors to be considered and those are climate change and the heavy use of manual labour, which could be scarce if another pandemic or catastrophic event happens, preventing people from working. Agriculture will also need to adapt to this, not only using IoT and AI but also using mobile autonomous robots, alone or as a collaborative system. These robots are used to perform manual labour tasks (seeding, planting, harvesting), acquire information about the fields through physical sensors or cameras built into the robots, and apply pesticides and disease control.

To execute most of these tasks like harvesting or seeding, some sort of [Unmanned Ground Vehicle \(UGV\)](#), like a tractor, is used. For the execution of other tasks like large area monitoring or the broadcasting of pesticides an [Unmanned Aerial Vehicle \(UAV\)](#), like a drone, is often used. These autonomous vehicles can handle tasks that humans would struggle to do more cheaply and quickly. However, these machines have a limited battery capacity and, therefore, need to be designed specifically for the task at hand. For instance,

in the case of UAVs, when covering a large area for monitoring, a lot of battery life is required. To facilitate this, the software and overall development of the robot need to be specialized [5, 6].

Going more in-depth into the design features, there are four main issues to consider: locomotion, sensing, planning, and manipulation. Starting with locomotion, there are various types of designs, including wheeled robots, flying robots, railed robots, wire-suspended robots, legged robots, and tracked robots which are used, for example, in wet environments where wheels might get stuck in the mud. When it comes to sensoring, it is also highly dependent on the task at hand. If the goal is to differentiate between two fruits with similar colours, a regular digital camera might not suffice, a more sophisticated camera with advanced image processing software may be needed. Additionally, some characteristics of the environment change, and therefore, the algorithms used must account for factors such as direct sunlight, temperature, and humidity. Moreover, planning is the list of decisions the robot has made to complete its task successfully. There are several algorithms used, however, the most advanced ones are the sample-based ones which have greater performance. Finally, manipulation is the control of manipulators, like robotic arms with grippers, to execute a certain task [7]. The choice of manipulator depends on the task, however, some robots have multiple manipulators, called **Multi-functional Intelligent Agricultural Robots (MIARs)**, to perform multiple tasks, [7] which reduces the number of robots and costs. Per [5, 6] some robots are also programmed to be able to perform multi-objective path planning which increases efficiency of movement in complex environments, increasing overall efficiency of the robot.

As an example, in [8], a robot was created to compensate the lack of labour caused by the aging of the population of Taiwan. The environment characteristics of Penghu, Taiwan, are prone to the overproduction of dragon fruit (Pitaya), and therefore this problem needs to be fixed to fight its production. Since the terrain is very shallow and has a poor water retainability, in addition to droughts, the soil has become arid which might make a wheeled robot bog down. The choice of locomotion for this robot were the tracks. For sensoring, a 9-axis gyroscope, to get the robots deviation, a Webcam (Image Sensor), to get the fruits location, and a Lidar to measure the distance between itself and any obstacle in its way. To harvest the fruit, it uses a 6-axis robot arm with a gripper end-effector. Finally, path-planning wise, it uses the 2-D SLAM algorithm to generate a pixel map and then the Dijkstra algorithm to calculate the fastest route to the target position. The experiments on the field revealed a 97% harvest success rate meaning the method used by the author is appropriate.

Another example of a solution is the robot in [9], a platform robot developed to try to compensate for the aging of the South Korea's population which is causing a lack of young labour. The robot was designed to work on a paprika greenhouse with a 3-meter-wide

corridor, where workers traverse, and 0.5-meter-wide ridge between crops where the robot will operate. The ridges between crops have hot water piping which serve as rails and therefore the robot was designed to be both railed and free driven. Its locomotion system consists of a two-wheeled drive kit with two main traction wheels in the middle, and four auxiliary smaller wheels to level the platform. Two in the front and two in the back. To move autonomously it incorporated a Lidar, to map the environment, a camera, to detect objects, and an encoder, to get the current position of the robot. The chassis was adapted to serve as a vacuum system, a lift table system or as just a manipulator. It had two controllers, one for the movement control system and another for the manipulation system. However, only the movement system was tested. This robot was not tested in the field, but, passed both the maximum load test (withstood 400Kg with no change of the distance between chassis and ground). The autonomous driving had some problems with the steering and network making it not ready to operate, however, it is a good start to solving this agricultural problem.

2.2 Motion Planning

Motion planning is of the most important steps to achieve autonomous movement in robots, and there are several methods that can be implemented to achieve this. The goal is to calculate a path that will get the configuration of the robot from a starting position q_{start} to a goal configuration q_{goal} , without colliding with any obstacle, and to achieve this there exist several methods. In [10, 11], the methods are divided into two categories, Classical Approaches, which include Cell Decomposition, Roadmapping, Sampling-based, and Bio-Inspired approaches, Roadmapping approaches, and the Learning Approaches which are the Supervised learning, Unsupervised learning and Reinforcement Learning based approaches. Additionally, according to [11], there are two types of planners, Global and Local planners. Global planning is when a path is planned with prior knowledge of the environment, whereas Local planning is when a path is planned reactively as the knowledge of the environment is being acquired in real time. Global planners focus on modelling method for the environment and path selection where Local planners focus on using data acquisition devices. Both types of planners can use the same approaches for path planning.

To continue there we'll need some definitions:

- C -space (C) are all the possible configurations the robot can have, for example in a robotic arm it is all the angles its joints can be in;
- C_{obs} are all the configurations where the robot is in contact with an obstacle;
- C_{free} are all the configurations possible for the robot to be in, but not in contact with an obstacle $C_{free} = C \setminus U C_{obs}$;

2.2.1 Cell Decomposition approaches

These approaches are called Grid-based because they divide the C-space into a grid where each centre point of a cell is a node. The path is chosen as a sequence of these nodes using algorithms like Dijkstra's algorithm or A* for example. There are three main types of Cell Decomposition approaches, the exact, adaptive and approximate cell decompositions [12].

2.2.1.1 Exact Cell Decomposition

The Exact Cell Decomposition approach divides the C-space into small polygonal elements formed by vertical lines created by every vertex of the obstacles. See Figure 2.1 for visual aid.

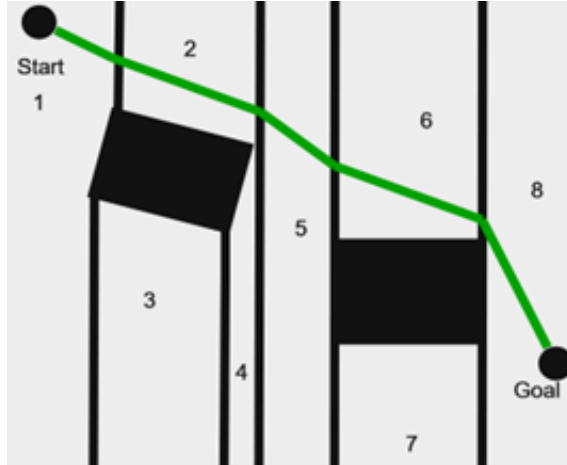


Figure 2.1: Exact Cell Decomposition representation;Green line is a possible chosen path.

2.2.1.2 Adaptive Cell Decomposition

The Adaptive or Quadtree Cell Decomposition approach firstly divides the C-space into four cells of the same size. Then every cell that is partially occupied will keep dividing itself until every cell is either free of obstacles or fully occupied. See Figure 2.2 for visual aid.

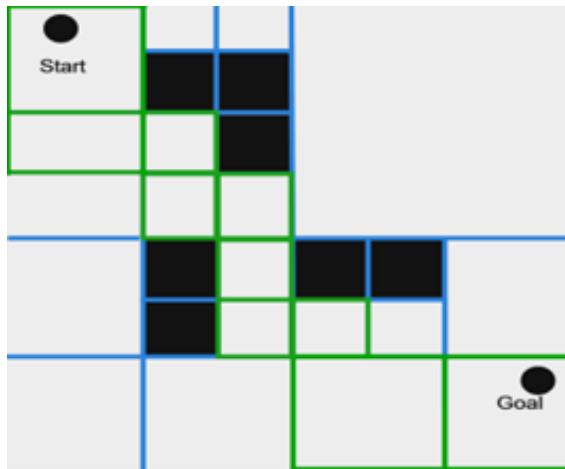


Figure 2.2: Adaptive Cell Decomposition representation; Green Squares are the chosen cells/nodes for the shortest path

2.2.1.3 Approximate Cell Decomposition

Finally, the Approximate Cell Decomposition approach simply divides the C-space into a grid with known cell size. The smaller the cells, better optimised the path, however, more combinations of path exist making computation more time consuming. There are two types of Approximate Cell Decomposition, 8-connected and 4-connected where the former accounts for diagonal movement between nodes and the latter only vertical and horizontal movement. See Figure 2.3 for 8-connected.

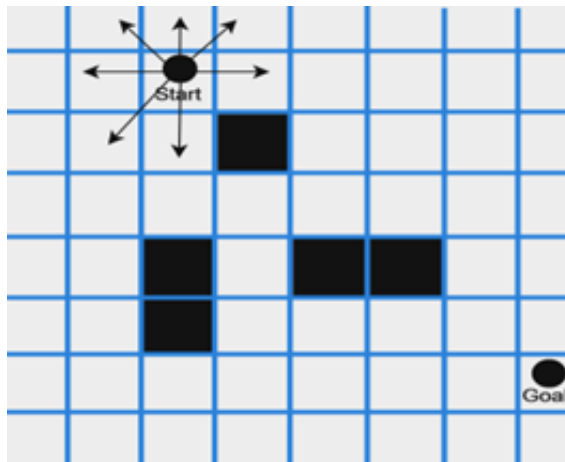


Figure 2.3: Approximate 8-connected Cell Decomposition representation; Arrows represent every possible movement the robot can make

2.2.2 Grid/Graph Search algorithms

Most of the motion planning approaches create graphs or grids where nodes are connected forming paths. After the paths are created the best one needs to be chosen. To make this choice, graph search algorithms are used. The most common ones are the Dijkstra's algorithm and the A* algorithm.

2.2.2.1 Dijkstra's Algorithm

Dijkstra's algorithm works by looking at the node with the shortest distance to the root of the graph, which in the beginning is the root itself. Then it calculates the distance to all the nodes connected to that node (every edge has a weight), and then chooses the node with the shortest distance to the root. Every node keeps track of the parent node and is updated if a shorter path to said node is found. This process is repeated until every node is visited. The path is then found by backtracking from the goal node to the root node.



Figure 2.7: 8-connected Dijkstra's Algorithm; a) is the starting C-space; b) is a mid point of the algorithm; c) is the end point of the algorithm; The green squares are the searched neighbours, the red ones are the visited nodes and the blue ones are the chosen path.

2.2.2.2 A* Algorithm

The A* is similar to the Dijkstra's algorithm, as it also goes from node to node calculating distances, however, it has a heuristic function that estimates the distance from the current node to the goal node. The value stored in each node instead of being the path distance from the root, is the sum of said distance and the estimated distance towards the goal.

$$f(n) = g(n) + h(n) \quad (2.1)$$

where $f(n)$ is the value stored in the node, $g(n)$ is the distance from the root to the node, and $h(n)$ is the estimated distance from the node to the goal. This way the chosen nodes are biased towards the goal, making the algorithm faster than the Dijkstra's.

The algorithm starts in the same way, calculates the f value for all the root adjacent nodes, chooses the smallest value, and then calculates the f value for all the nodes connected to the chosen node. This process is repeated until the goal node is reached. If a value is found that is smaller than the one stored in the node, the value is updated. The path is then backtracked from the goal node to the root node.

As seen in Figure 2.11, the path has more diagonal transitions than the one in Figure 2.7, making it slightly longer. This is due to the heuristic function used in the A* algorithm which makes it go faster towards the goal, but not always in the shortest path.



Figure 2.11: 8-connected A* Algorithm; a) is the starting C-space; b) is a mid point of the algorithm; c) is the end point of the algorithm; The green squares are the searched neighbours, the red ones are the visited nodes and the blue ones are the chosen path.

2.2.3 Artificial Potential Field

The traditional [Artificial Potential Field \(APF\)](#) approach consists of assigning a positive potential to obstacles and a negative one to the end state. Using the robot as a positive charge, the end goal will have an attractive force on the robot while the obstacles a repulsive force. This way the robot is attracted to the goal configuration while being repelled by the obstacles. This method is advantageous due to its simplicity [13] and due to its speed when compared to the graph search algorithms [14]. However, the main problem with this algorithm is its susceptibility to the local minima problem [13, 14]. If there is ever a configuration where the repulsive forces generated by the obstacles are symmetrical to the attractive one of the goal state, the robot will not be able to move.

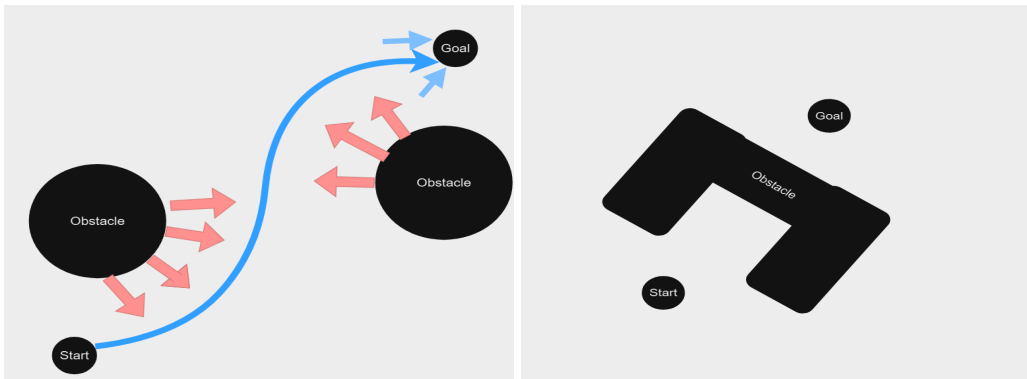


Figure 2.12: APF algorithm; On the left is the normal functioning of the algorithm where the pink arrows represent obstacle repulsion, the smaller blue ones represent the goal attraction and the curvy blue arrow is the chosen path; On the right is the local minima situation.

To solve this local minima problem, the author in [15] proposed a solution where when the robot is detected to be facing this problem, it will move in a random forward direction to get out of that situation. Another approach is to combine multiple methods like the author of [16] proposed. His approach was to use the traditional APF until a local minima

position is reached and then switches to using the RRT*, a sampling-based algorithm explained in 2.2.4.2, to escape it.

2.2.4 Sampling-based approaches

There are two main sampling-based approaches, the [Probabilistic Roadmap \(PRM\)](#) and the [Rapidly-exploring Random Tree \(RRT\)](#). These algorithms sample the C-space creating nodes and then connecting them forming a roadmap.

2.2.4.1 Probabilistic Road Map

The [PRM](#) is divided into two phases, being the construction and query phase. The construction phase starts by sampling the C_{free} and establishing feasible or non-obstructed connections between the sampled nodes, creating a roadmap R. The query phase joins the initial and goal configurations to the roadmap by connecting them to the closest non-obstructed nodes and then, by using, for example, a distance-reduction algorithm like the A* or Dijkstra, obtaining the desired path. This approach has difficulty in narrow environments because of its probabilistic nature it is not certain that the sampled nodes can make connections.

In [17] this technique is used along with the [APF](#) approach and the Approximate Cell Decomposition approach creating the HPPRM or Hybrid Potential Based Probabilistic Roadmap, to avoid the problem mentioned. It first creates a Potential map with the obstacles' information, then it divides the map into a grid with cells with the same size. Afterwards classifies the cells into High or Low potential depending on the repulsive values calculated. Higher potential cells would have more samples than lower potential ones since making connections in the latter would be easier. After having the nodes, the process is the same as the one in [PRM](#), connections between nodes are made and then the Dijkstra's algorithm is used to obtain the shortest path between initial and goal configurations.

2.2.4.2 Randomly Exploring Random Trees

The other method, the [RRT](#), consists of, with the starting configuration as the root of the tree, randomly sampling the C_{free} and creating a node that connects to the nearest one until the end goal is reached. The creation of the node isn't always on the sample but within a maximum distance in the direction to the nearest node. Once the end goal is reached, all needed to do to get the path is to follow the only path from root to goal state. Despite always being able to find a feasible path, as samples approach infinity, this method as an issue, since the samples are random, the path created might not be optimal in a distance sense. As a solution to this problem, the RRT* algorithm was created. The node creation process is the same as the [RRT](#), a sample is randomly generated, find the nearest node, create a node within the maximum distance from the nearest node and the

sample. The difference is in the connection to the tree, instead of connecting it to the nearest node, it searches the nodes around it, within a certain range, and checks if they can be rewired so that the paths are shorter. The sampling ends when a short enough path is found, or the number of samples reaches the desired amount. There is also another variation of RRT which is the bidirectional RRT which works exactly like the RRT but both goal and starting configurations start as a root to a tree, expanding towards each other.

In [18], a combination of variations of the RRT are used. The author mentions the use of the Bi-RRT to find, in less time, a feasible path between the starting and goal configurations. However, due to the algorithm's random nature and robot's constraints, the connections between the two trees are made by solving a 2-point Boundary Value Problem which may take too much time in a practical scenario. To get around this issue, the author proposed the use of a bidirectional-unidirectional-RRT which functions as a regular Bi-RRT with the two trees growing into each other, but, when close enough to connect, it will use a unidirectional search, starting from the initial configuration's tree, with a bias towards the goal state's tree.

2.2.5 Roadmapping approaches

The Roadmapping approaches are divided into main two types, the Visibility Graphs and the Voronoi Diagrams which are motion planning approaches that form connections creating roadmaps.

Note: The PRM and RRT approaches weren't included in this section due to their stochastic nature. For the same C-space there can be multiple roadmaps using PRM and RRT, whereas in the Visibility Graph and Voronoi Diagram approaches there is only one.

2.2.5.1 Visibility Graph

Visibility graphs function by representing every object as a polygon and then connecting every adjacent vertex, including starting and end points, forming straight lines that do not go through objects. Once multiple connections are formed an optimal path is chosen using an algorithm like A* or Dijkstra's. However, this approach has the problem of being time complex and not being dimensionally scalable [19].

An example of the usage of this method can be seen in [20] where the visibility graph approach is used for in real time obstacle avoidance for a UAV. However, due to mechanical restraints the aircraft needed the connections between edges to be smoother, and therefore used the Dubins curves method, which makes a path from A to B using a sequence of straight and curved lines with a minimal R radius imposed by the necessary restraints [21]. Another example of the use of this approach is in [22] where the author used the Visibility Graph and the Adaptive or Quadtree Cell Decomposition methods to create a path for a marine USV for the coast of South Korea. The map was divided into a grid with

four cells, NW, NE, SW, SE, and then would be divided like explained in 2.2.1. After the construction of the quadtree graph, the visibility graph is created using the nodes in the centre of each cell. The shortest path is then chosen using the Dijkstra's algorithm.

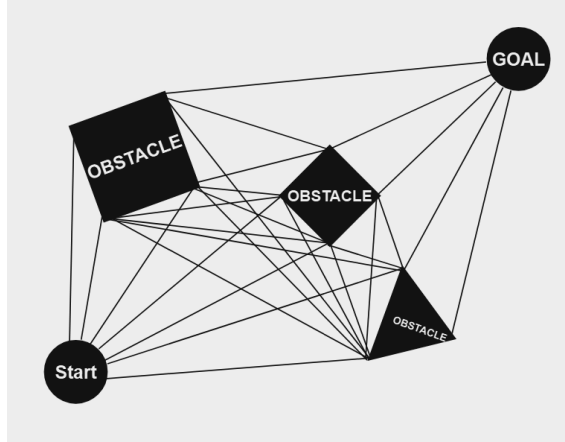


Figure 2.13: Visibility Graph representation; As explained, the black lines are the connections between the vertices that will then be searched for the shortest path

2.2.5.2 Voronoi Diagram

The Voronoi Diagram consists of two sets, the vertex or node set, and the edge set. The edge set is the collection of all the lines which are equidistant to two objects, and the vertex set is the collection of all the points where three or more lines intersect. These objects may be obstacles or just workspace boundaries. Again, like in the Visibility Graphs, after the diagram is created, the best path can be chosen using an algorithm like A* or Dijkstra.

The usage of this approach can be exemplified in [23] where the author used the Voronoi Diagram along with the RRT* and Potential Field approaches to create a path for a [UGV](#) in an indoors environment. Firstly, the planner would create a Voronoi Diagram of the C-space, however This would not suffice for a successful path plan due to the robot's mechanical constraints. For this, a potential function was used to create a map where the most attractive points would be in the path chosen using the Voronoi Diagram. Afterwards, the RRT* algorithm was used to create the optimal path sampling with a bias towards the attractive field. Despite this approach being successful in most cases, there were still cases where the robot's dynamics would prevent it from following the desired path. The author then suggests that this problem would easily be overcome by making a circle around the robot and if the circle isn't able to move in that position, the position would be discarded, and another path would be chosen in the Voronoi Diagram phase.

2.2.6 Bio-Inspired approaches

The Bio-Inspired approaches are, as the name would suggest, inspired by natural systems. The main methods are the [Ant Colony Optimization \(ACO\)](#), [Particle Swarm](#)

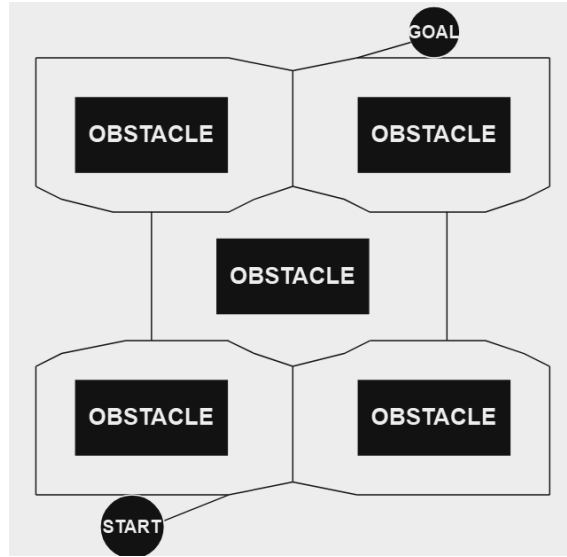


Figure 2.14: Voronoi Diagram representation; The black lines keep the same distance to the obstacles and the map edges

[Optimization \(PSO\)](#) and the [Genetic Algorithm \(GA\)](#). These optimization algorithms minimize a specific Objective or Cost function, which could factor path length, energy spent, or any other example specific characteristic that could impact performance [24].

2.2.6.1 Particle Swarm Optimization

The [PSO](#) algorithm starts by creating a swarm of particles, each with a position and velocity. In the motion planning context, each particle represents a possible solution or, in other words, a feasible path. The particles' position and velocity are updated, with each iteration, according to the following equations:

$$v_i^{t+1} = w v_i^t + c_1 r_1 (pbest_i - x_i^t) + c_2 r_2 (gbest - x_i^t) \quad (2.2)$$

$$x_i^{t+1} = x_i^t + v_i^{t+1} \quad (2.3)$$

where v_i^t is the velocity of particle i at time t , w is the inertia weight, c_1 and c_2 are the cognitive and social coefficients, r_1 and r_2 are randomly generated values between 0 and 1, $pbest_i$ is the best position of particle i , and $gbest$ is the best position of the swarm. The algorithm stops when a maximum amount of iterations K is reached.

This approach was used in [25] the author defined the particles as a set of parameters of cubic splines, which would connect to form a smooth path for the robot. The cost function used considered the path length, the minimum distance between the robot and the closest obstacle, and the Euclidean distance between the robot and the goal configuration. This method was compared to the visibility graph and the [APF](#) and found that it was able to find a smoother and more easily executable path (less discontinuities) while maintaining a short path distance. Due to how slow the algorithm is, the author says that it can only be used in a static environment.

2.2.6.2 Ant Colony Optimization

The ACO algorithm is inspired by the behaviour of ants when looking for food. When traveling, ants leave pheromone trails so the other ants can follow them. The algorithm tries to mimic this behaviour by creating a set of artificial ants that will create a path from the starting to the goal configuration. The probability of a k ant of going from node i to node j at time t is given by the following equation:

$$P_{ij}^k = \frac{\tau_{ij}^\alpha(t) \eta_{ij}^\beta(t)}{\sum_{k \in N_i} \tau_{ik}^\alpha(t) \eta_{ik}^\beta(t)} \quad (2.4)$$

where N is the set of nodes connected to i , τ is the pheromone level of the path from i to j , η is the heuristic information or proximity, α is the pheromone incentive factor which means that the larger the α the more weight the pheromone level has on the probability of a path being chosen, and β which acts the same way as the previous coefficient only not for pheromone level but for proximity between nodes [26]. The pheromone level is updated at the end of each iteration using the following equation:

$$\tau_{ij}(t+1) = (1 - \rho)\tau_{ij}(t) + \rho\Delta\tau_{ij}(t) \quad (2.5)$$

where ρ is the pheromone evaporation rate and $\Delta\tau_{ij}$ is the increment amount of pheromone left by the ants in the path from i to j . Given a maximum number of iterations, naturally the shortest path will be the one with the most pheromone left by the ants. Due to its robustness, global optimization ability, and possibly being used in combination with different heuristic algorithms, the ACO is widely used in path planning. However, in complex environments, the algorithm may get stuck in a local minima or get into a Deadlock state where the ants can't escape from a specific node as there are not any explored ones nearby [27].

In [28] the author proposes an improvement to the ACO algorithm to plan a path in a radioactive environment. The proposed method added a chaos optimization algorithm to create initial random initial paths, it changed the pheromone update equation to include radiation level as a negative trait and also added a local search optimization to avoid the local minima problem. This method proved to be more efficient than the traditional ACO and PSO algorithms in the same scenario.

2.2.6.3 Genetic Algorithm

This method is inspired on the evolution of species. The algorithm starts by creating a random population of chromosomes, each representing a possible solution to the problem, like in the PSO. With every iteration each chromosome is evaluated using a fitness function, which is the cost function in the motion planning context. The better performing chromosomes have increased chances of being selected for reproduction. The

reproduction process is done by selecting two chromosomes and crossing them over, creating a new chromosome. This new chromosome can be mutated in order to create different solutions and therefore diversity. The process is repeated until a maximum amount of iterations is reached or a desired fitness level is achieved.

An improved version of this method was used in [29] to plan a path for an Unmanned Surface Vehicle. The chromosome encoding was done using sets of angles and velocities (θ, v) creating one hour steps. In the traditional GA, mutation is done by replacing a parent gene with a random value. The author believes that this approach is not optimal suggesting an alteration to the formula by taking the previous value and adding a value dependent on the gene's position multiplied by a random value and a constant. This change in the approach makes it so the mutated child will be closer to the parent, making convergence faster. The fitness function used is a Monte Carlo approximation of the cumulative detection probability which calculates the efficiency of a path. This method showed better results than the traditional GA as it had faster convergence to the optimal value and was also faster.

2.2.7 Learning-based approaches

There are three main types of learning based approaches, Supervised, Unsupervised and Reinforcement learning [30].

2.2.7.1 Supervised Learning

The Supervised Learning methods, like most ML approaches, are used to predict a value based on a trained model. To train this model a labelled and classified dataset is needed. The model is then trained based on the provided data and is used as necessary. The most commonly used Supervised Learning methods are the artificial neural networks, and the [Support Vector Machines \(SVM\)](#), however, methods can be used like linear regressions, randomforest, logistic regressions, convolutional neural networks, recurrent neural networks, K-nearest neighbour, and Naïve Bayes [30].

2.2.7.2 Unsupervised Learning

The Unsupervised Learning methods function similarly to the Supervised Learning methods, however, there is no labelling or classification of the datasets. The models are trained to find clusters or patterns in the data [31]. Due to this difference the dataset usually needs to be larger than the one used in Supervised Learning methods [30].

2.2.7.3 Reinforcement Learning

The Reinforcement Learning methods, much like the unsupervised ones, do not get a labelled or classified dataset to be trained on. Instead the model is trained by trial and

error, where the model is rewarded or punished based on the arrived state [32].

Examples of the usage of Learning-based approaches can be found in [33] where the author used a Reinforcement Learning approach to generate actions the robot should take to reach the desired configuration. Another example can be found in [34] where the author proposed a new method combining Convolutional Neural Networks and the RRT* algorithm, and concluded that the new method outperformed the conventional RRT* algorithm in the same scenario.

2.3 Motion Control

With a path calculated, the next step is to make the robot follow it, for this we use a robot controller or path tracker. In this section, the most common path tracking controllers will be explored, and these controllers are the [Pure Pursuit Controller \(PP\)](#), the [Model Predictive Controller \(MPC\)](#), and the [Dynamic Windows Approach \(DWA\)](#) [35].

2.3.1 Pure Pursuit

The algorithm works by calculating an arc between the robot's nearest waypoint and the one that is at least a lookahead distance L away [35]. Assuming the Path as a set of waypoints $P = p_0, p_1, p_2, \dots, p_n$, the point nearest to the robot is chosen as p_r and the lookahead point p_l is chosen as follows:

$$dist(p_i) = \sqrt{(x_r - x_i)^2 + (y_r - y_i)^2} \quad (2.6)$$

$$p_l = p_i \in \mathcal{P}_t, \quad \begin{cases} dist(p_{i-1}) < L \\ dist(p_i) \geq L \end{cases} \quad (2.7)$$

with a chosen p_l it is now possible to calculate the curvature of the arc that will be followed by the robot:

$$\kappa = \frac{2y'_l}{L^2} \quad (2.8)$$

where y'_l is the lookahead's point lateral coordinate and L the desired distance between the robot's point and p_l . This algorithm assumes a constant velocity and lookahead distances and, therefore, to improve performance in more complex scenarios, a new version of this controller was created, the Adaptive Pure Pursuit, where the lookahead distance is proportional to the current velocity:

$$L_t = v_t \cdot l_t \quad (2.9)$$

where L_t is the lookahead distance at time t , v_t is the current velocity, and l_t is the lookahead gain.

2.3.2 Model Predictive Controller

The [MPC](#) is a control method that uses the model of the robot system to optimize a cost function. The controller works by, given an Horizon N, predicting the future states of the robot and then minimizing the cost function to obtain the optimal control inputs for the states in the horizon. The controller keeps iterating this process, predicting the future states and optimizing control action until the goal configuration is reached.

The cost function will vary from case to case but in a path tracking problem can be defined as [36]:

$$J(\Delta \mathbf{U}, \mathbf{e}) = \frac{1}{2} \left\{ \sum_{i=k+1}^{k+N_p} \|\mathbf{e}(t_i)\|_Q^2 + \sum_{i=k+1}^{k+N_c} \|\Delta \mathbf{u}_e(t_i)\|_R^2 \right\} \quad (2.10)$$

where $e(t_i)$ is the error between the reference point and the robot's current position, $\Delta u_e(t_i)$ is the increment of the control input, the N_p and N_c are the prediction and control horizons, and Q and R are the weighting matrices for the error and control input increment, respectively. Additionally, the control action can be constrained by the robot's physical limitations, like maximum and minimum velocity, acceleration, and jerk.

2.3.3 Dynamic Window Approach

The [DWA](#) works by, like in the [PP](#), creating arcs the robot will follow. Firstly, it generates circular trajectories with different pairs of velocities and angular velocities. Then it chooses the only pairs which allows the robot to stop before reaching an obstacle. Finally, it applies the dynamic window where it eliminates the pairs in which the required velocities aren't reachable in the chosen time period. After eliminating all the non usable pairs, the pair with the smallest value when the cost function is applied is chosen as the control action [37]. The cost function can be defined as:

$$J(v, w) = \alpha \cdot \text{heading}(v, w) + \beta \cdot \text{distance} + \gamma \cdot v \quad (2.11)$$

where α , β , and γ are the weighting factors, the heading is cost of the difference between where the robot is facing and the desired node direction, the distance is cost of the distance between the robot and the closest obstacle, and v is the robot's velocity. This process is repeated between nodes until the goal configuration is reached.

2.4 Localization and Mapping

In order to obtain a path for the robot to follow, it is imperative that the robot knows where its initial and goal configurations are, and also the position of the obstacles around the world. To achieve this two things need to happen, Mapping, to get a representation of the world, and Localization, to know where the robot is relative to the obstacles and the goal configuration.

2.4.1 Localization

Localization is the process of determining the robot's position and orientation in the world. This process can be done using different methods, motion sensors that give speeds, accelerations and orientations, Vision sensors that can get information about the robotics surroundings, however, it is not possible to use these sensors alone as they can be noisy [38] and, therefore, Kalman Filters are used to fuse the information from the different sensors and get a more accurate position. This method is called Odometry.

Odometry alone cannot be used to get the robot's position as it is prone to drift over time [39], and therefore, other methods are used to correct the accumulated error. One of the most common methods is the [Adaptive Monte Carlo Localization \(AMCL\)](#). This method uses a particle filter to achieve a more accurate position, however, it requires a considerable amount of computational power and memory, as accuracy improves with particle count [40]. To solve this, both Odometry and [AMCL](#) are used together, where the Odometry is used to get a continuous estimation of the robot's position and is then, periodically, corrected by the [AMCL](#) which uses a map of the world to get a more accurate position.

2.4.2 Mapping

Mapping is the process of creating a 2D representation of the world and can be achieved using algorithms like the [Simultaneous Localization and Mapping \(SLAM\)](#), where both the map and the robot's positions are estimated at the same time, making it a very complex problem [41]. There are a few different solutions to this problem, the probabilistic approaches, such as the Kalman Filter, the Particle Filter and Information filter [41], that are created from the Baye's Rule. [SLAM](#) is a very popular topics in robotics and there has been improvements to the traditional approaches like the more recent Visual-SLAM or VSLAM which also use images to facilitate obstacle detection and tracking [42].

2.5 Related Work

Since the system that this thesis will be focusing on is a tractor-trailer system, in this section there will be a brief explanation of the system and some ways it's been approached.

2.5.1 System Description

The tractor-trailer system is a system where a self-propelled vehicle, the tractor, pulls a non-propelled vehicle, the trailer. This system has been modelled in many papers and generally takes the following form [43, 44]:

$$\dot{x} = v \cos(\theta_0) \quad (2.12)$$

$$\dot{y} = v \sin(\theta_0) \quad (2.13)$$

$$\dot{\theta}_0 = \frac{v}{WB} \tan(\phi) \quad (2.14)$$

$$\dot{\theta}_1 = \frac{v}{RTR} \sin(\theta_0 - \theta_1) \quad (2.15)$$

where x and y are the hitch position, v is the robot's velocity, θ_0 is the tractor's orientation, θ_1 is the orientation of the trailer, ϕ is the steering angle, and WB and RTR are the wheel base distance (distance between axles) and the distance between the hitch and the trailer's rear axle, respectively.

2.5.2 Applications

Some applications of the tractor-trailer system can be found in [43], where the author proposed a Voronoi Hybrid A* for the path-planner and two pure-pursuit controllers as path trackers. The author concluded that the traditional approaches were not feasible due to generating paths that wouldn't account for the trailer's non-holonomic constraints. Therefore, a different version of the A* was used. The Hybrid A* is much like the traditional one, however, instead of only being able to move to the nodes or grid cells, the nodes generated in the Hybrid A* contain the robot's dynamics $(x, y, \theta_0, \theta_1, d)$ where d is the direction of motion of said node (forward or reverse), and can reach anywhere in the continuous state space. The cost of each node is calculated penalizes the change of direction, backwards movement, steering input, change of steering input, jack-knifing and path length. Since these nodes have discrete values, it is not possible to always reach the desired nodes, therefore, the author used a Dubins curve to connect waypoints generated by a traditional A* search on the Voronoi Graph. This approach was compared to the Hybrid A* without the Voronoi Graphs and the Voronoi Hybrid A* was able to create slightly shorter paths a thousand times faster. With a generated path, the author used two pure pursuit controllers that switched depending on the direction d of a node. This approach to the tractor-trailer problem was able to manoeuvre in tight indoor environments which is a necessary feature in the context of this thesis since greenhouse and farm corridors are typically narrow. This approach is also successful because it takes a relatively short time to generate a smooth path, however, it does not include a local planner for dynamic environments which may be crucial in a real-world scenario where workers or other robots may be present.

Another application of the tractor-trailer system can be found in [45] where the author created a path tracker using an mpc controller. The systems model is slightly different from the previous as the author used both the translational velocity and the angular velocity as control inputs $u^T = [v, w]$. The system's dynamics become the following:

$$\dot{x}_1 = v \cos(\theta_0) \quad (2.16)$$

$$\dot{y}_1 = v \sin(\theta_0) \quad (2.17)$$

$$\dot{\theta}_0 = w \quad (2.18)$$

$$\dot{\theta}_1 = -v \frac{1}{l_2} \sin(\theta_1 - \theta_0) + w \frac{l_1}{l_2} \cos(\theta_1 - \theta_0) \quad (2.19)$$

where x_1 and y_1 are the tractors centre position, l_1 is the distance between the tractor's front axle and the hitch, and l_2 is the distance between the hitch and the trailer's rear axle.

The obstacles, walls and the robot were expressed as polygons to facilitate the collision avoidance as this approach has no path planner, only a few hand placed waypoints. With these polygons, the Farkas' lemma to create a constraint for the mpc controller by expressing the polygons as two matrices A and b to discretise the obstacles position and orientation.

The cost function created took into consideration the deviation from the goal state, the deviation from the reference translational velocity and the variation of input control:

$$J = x_e^{goal}(N)^T S x_e^{goal}(N) + \left(\sum_{i=0}^{N-1} x_e^{goal}(k)^T Q_1 x_e^{goal}(k) + v_1 e^{ref}(k)^T Q_2 v_1 e^{ref}(k) + \Delta \hat{u}^T(k) Q_3 \Delta \hat{u}(k) \right) \Delta \tau \quad (2.20)$$

where x_e^{goal} is the error between the goal state and the current state, $v_1 e^{ref}$ is the error between the current velocity and the reference velocity, $\Delta \hat{u}$ is the control input increment, and $\Delta \tau$ is the time step. The controller was constrained by the robot's physical limitations in u^{min} and u^{max} and the obstacle avoidance equation. This cost function is minimised in every iteration until the horizon N is reached.

This approach to path tracking was tested using a narrow environment with four waypoints that would appear one by one as the robot reached them. The testing occurred in two phases, one being in a static environment and the other in a dynamic one. In the first one the robot was able to reach the goal while managing tight curves and counter curves. However, in the second phase, the robot encountered a problem when the dynamic obstacle was placed in front of the robot, as the robot couldn't avoid it and had to reverse to avoid a collision. This happened because the obstacle wasn't considered dynamic by the model and couldn't predict its movement.

Overall, this approach was able to reach the waypoints without collisions and is very promising, however, it does not have a path planner to place the waypoints and has to be done by hand. It starts to tackle the object avoidance issue to some successful extent but could be improved.

In [46] an exact local planner was used to solve this problem. The tractor-trailer is a non-holonomic system that can't be integrated, however, if the steering angle and velocity were constant, the system would now be integrable. The author used this concept to create rotational and translational paths for this system. Since the steering angle is constant and constrained by the vehicles dynamics it was possible to calculate the angle for each arc by using the following equation:

$$\phi = -\arctan\left(\frac{L_1 \sin(\theta_1)}{L_2}\right) \quad (2.21)$$

where L_1 is the distance between the hitch and the tractor's front axle, L_2 is the distance between the hitch and the trailer's rear axle, and θ_1 is the orientation of the trailer. This approach resembles a PP as it also calculates the curvature of the arc needed for a smooth path. The paths between two nodes are created by connecting two rotational paths and one translational path, this means, two arcs around the nodes and one straight line connecting them. The author mentions that this method can't deal with obstacle avoidance, however, if a global planner was integrated, this wouldn't be a problem since the nodes would be placed in a way that connections would be collision free. The testing revealed that this approach could generate a feasible and smooth path in under two seconds, which for the time (1995) was quite a fast time. This approach wouldn't suffice for this thesis' problem as a whole, however could be used as a path tracker instead of a path planner.

In [47], the authors present a unified trajectory planning and tracking framework for autonomous tractor-trailer vehicles by integrating APF into MPC. The APF models environmental interactions with attractive forces toward the goal and repulsive forces from obstacles, which are embedded into the MPC objective function to ensure dynamic feasibility, collision avoidance, and adherence to kinematic constraints. The method is tested in Matlab/Simulink simulations covering overtaking, obstacle cut-ins, emergency braking, and multi-obstacle avoidance. The results demonstrate robust collision-free navigation and smooth trajectory execution, outperforming geometry-based planners in stability and optimality, though it assumes low-speed maneuvers where kinematics suffice. Despite its apparent success, this method does not deal with the problem of recovery manoeuvres in the case there is a need for reversing, which is a common situation in narrow and complex environments.

Another example of path planning for tractor-trailer systems can be found in [48], where the authors propose an optimization-based algorithm targeting on-road scenarios for articulated vehicles composed of a tractor and a trailer, like transport trucks. The vehicle is modeled in a road-aligned coordinate frame to suit on-road planning, incorporating driving heuristics into various optimization objectives aimed at minimizing the distance the tractor and trailer deviate from the original path while staying on the road and avoiding obstacles. The approach is evaluated in simulations on challenging on-road scenarios using demanding tractor-trailer dimensions. Results show that the planner computes paths that effectively reduce off-tracking, with certain objectives performing better in tight maneuvers like roundabouts, though computation times vary and some scenarios require tuning to avoid infeasible solutions. This method, while effective in on-road scenarios, may not be directly applicable to the agricultural context of this thesis, where environments may be more dynamic and may require .

2.6 State of the art Summary

To summarize, the tractor-trailer pesticide spraying robot proposed in this dissertation could be of help in the agriculture industry, and, to develop this project there are several approaches to be considered. Various methods for path planning and control in tractor-trailer systems have been explored in the literature. For instance, optimization-based planners like those in [48] focus on on-road scenarios, minimizing off-tracking through heuristics and objectives tailored to articulated vehicles, performing well in simulations of tight maneuvers such as roundabouts but requiring parameter tuning and potentially facing infeasibility in complex cases. Similarly, unified frameworks integrating APF with MPC, as in [47], enable simultaneous planning and tracking, handling dynamic obstacles in simulations like overtaking and emergency braking, though they may not address reverse maneuvers essential for narrow agricultural spaces. Other approaches include MPC-based trackers with manual waypoints [45], which manage static and dynamic environments but rely on predefined points and don't adapt the plan if there is a change in the environment, and exact local planners using constant steering for integrable paths [46], generating quick feasible paths but lacking inherent obstacle avoidance without a global planner. When it comes to path planning, the Hybrid A* algorithm is a good choice as its nodes are placed in a way that allows for safe navigation where the trailer will not jackknife, this algorithm could be used in combination with the Voronoi Graphs to create a faster path by having a precomputed graph that the Hybrid A* can be ran on, like in [43]. To control the robot, the most used options would be the optimal control controllers like the [MPC](#), as it can predict future states and optimize the tracking problem, however, this approach could be overkill if the path is already calculated. The next best option for a rover would be the [PP](#), as it is simple to implement, calculates the velocities for the robot to follow arcs, which is what the planer is being designed to account for. It can reduce the tractor-trailer problem into just a car problem by having steering and velocity as constant values. For a local planner, in case a dynamic object appears in front of the robot, the [MPC](#) could now be used to reach the next node in the path, as it could take too much time for a complete replan of the path, however, if safety is a priority, overtaking an obstacle is not a must, stopping and waiting for a replan is a valid option. This project is a very important one, as there isn't a lot of documentation on solutions for this problem, and especially in the context of Smart Agriculture.

ARCHITECTURE

In this chapter there will be a presentation of the architecture of the proposed solution as well as some insights into its implementation.

3.1 System Overview

The proposed solution is designed to address the complexities of navigating a tractor-trailer system in narrow environments, such as agricultural fields. This system integrates advanced path planning and control strategies to ensure safe practices, with collision avoidance, and effective navigation, tending to the specific needs of this type of system.

The system is divided into two main components: a self-propelled tractor and a non-propelled trailer. The tractor is a four-wheeled differential driven robot that serves as the navigation and propulsion unit. The trailer, designed for modularity can have its own independent functionalities allowing for a simpler maintenance and adaptability to different tasks. This modularity allows for the independent development of the tractor's navigation and control systems without the need of knowing the trailer's payload or functionalities, with perhaps the exception of the trailer hindering the sensor's view or the trailer's weight exceeding the tractor's capabilities.

The solution proposed in this work is divided into four main modules:

- **Environment:** This module is responsible for the representation of the real world, or actually be the real world. This is where the robot will operate.
- **Sensor perception:** This module is responsible for gathering data from the environment and converting it into usable information like localization and estimation.
- **Path planning:** This module is responsible for generating a feasible path from the current position to the desired goal.
- **Control:** This module is responsible for tracking the generated path and ensuring the tractor-trailer system follows it safely without collisions.

From the modules mentioned above, the ones that are implemented in this work are mainly the path planning and control modules, however, in order to test and develop the system, the environment and sensors were simulated.

The overall functioning of the system is as follows: the tractor is at a point in the environment, simulation or real world, the user then requests a movement to a specific position, the path planning module will then generate a path from the current position, estimated with sensor gathered data, to the desired goal. The path is then forwarded to the controller which will then track it by computing the necessary angular and linear velocities while ensuring the physical constraints of the tractor-trailer system are respected.

3.2 Planner

The planner is a Voronoi Hybrid A* mixture which takes the ability to generate feasible paths from the Hybrid A* and the added velocity of having a pre-computed Voronoi graph to expand from.

The following flowchart shows the logic of the planner, starting with the request for movement, assigning a goal target. Then, the planner will perform an A* search on the pre computed Voronoi Graph, starting from the current robot position, to the goal pose. The A* search will return a path which consists of a series of subgoals which will later on be used to speed up the path creation process. Having the subgoals, the next step is to try and find a feasible path from the current position to the subgoal nearest to the goal pose, in this case, since it is the first iteration, the actual goal. If the path is feasible, then the planner will simply return said path, otherwise the planner will try to do the same but with the next subgoal, until it either finds a feasible path or exhausts all the subgoals. If it finds a path, it will repeat the previous process, but instead of using the current position as the starting configuration, it will use the subgoal which a path was able to be computed to. If it exhausts all the subgoals, then it will try and compute a new node, a Hybrid A* node, which consists of a segment, starting from the current algorithmic position (can be the start point or a subgoal depending if a path was found previously), to any point that is reachable by the tractor at a distance d defined by the user, and then assign them as the current algorithmic position to run the Dubins loop again.

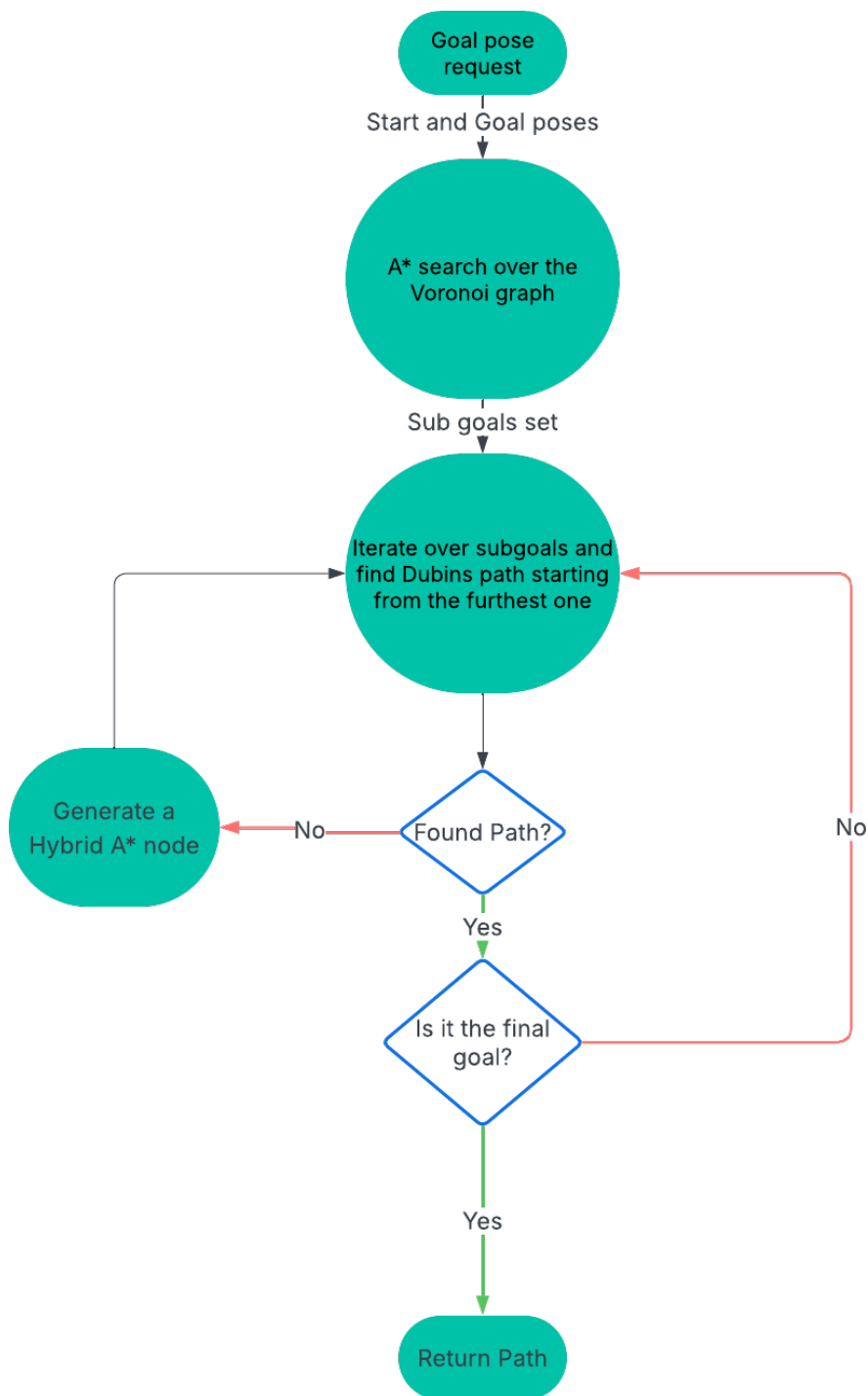


Figure 3.1: Planner logic flowchart

Algorithm 1 Planner Pseudocode

```

1: function GET_PATH(start, goal)
2:   subgoals  $\leftarrow$  get_subgoals(start, goal, voronoi_graph)
3:   current  $\leftarrow$  start
4:   path  $\leftarrow$  None
5:   for all subgoal in subgoals do
6:     path  $\leftarrow$  get_feasible_path(path, current, subgoal)
7:     if path  $\neq$  None then
8:       if subgoal = goal then
9:         return path
10:      else
11:        current  $\leftarrow$  subgoal
12:      end if
13:    end if
14:   end for
15:   while True do
16:     new_node  $\leftarrow$  expand_hybrid_node(start)
17:     if check_not_feasible(new_node) then
18:       return None
19:     end if
20:     path  $\leftarrow$  attach_node_to_path(path, new_node, goal)
21:     current  $\leftarrow$  new_node
22:   end while
23: end function

```

Algorithm 1 shows the detailed pseudocode for the planner. Starting with the subgoals generation, to the looping through them and trying to find a path, to, if needed, the expansion of the hybrid A* nodes.

Algorithm 2 shows the pseudocode for the subgoal generation, which is done by performing a regular A* search on the pre-computed Voronoi graph. It starts by examining the neighbours of the start node and adding them to the open list, it then goes through the open list and performs the same operation until the goal is found or the open list is empty.

The Dubins path creation is more mathematically complex to represent simply in pseudocode. It is a calculation of forwards segments that can be of 6 different types, Left Straight Left (LSL), Left Straight Right (LSR), Right Straight Left (RSL), Right Straight Right (RSR), Right Left Right (RLR) and Left Right Left (RLR). These paths are the shortest possible curves connecting two configurations for a non-holonomic vehicle with a fixed minimum radius. The process is divided into six main steps, normalizing the problem, by calculating the distances between start and goal configurations and also the orientation, the start heading from start to goal and the goal heading relative to the line connecting the start and goal. The next step is to compute the six paths, one of each type and check their feasibility, then, the feasible paths are sorted by length and the shortest is the chosen one. Finally, the path is then segmented into short segments of (x, y and yaw) and then returned.

Algorithm 2 Get_subgoals Pseudocode

```

1: function GET_SUBGOALS(start, goal, voronoi_graph)
2:   subgoals  $\leftarrow$  []
3:   closed_list  $\leftarrow$  []
4:   open_list  $\leftarrow$  [start]
5:   found  $\leftarrow$  False
6:   while open_list.not_empty() and not found do
7:     current  $\leftarrow$  open_list.pop()
8:     closed_list.append(current)
9:     neighbours  $\leftarrow$  current.neighbours
10:    for all neighbour in neighbours do
11:      if neighbour not in closed_list then
12:        if neighbour in open_list then
13:          if current.f < open_list(neighbour).f then
14:            continue
15:          end if
16:        end if
17:        current.parent  $\leftarrow$  current
18:        current.f  $\leftarrow$  compute_fcost(current, neighbour, goal)
19:        open_list.append(neighbour)
20:      end if
21:      if neighbour is goal then
22:        goal.parent  $\leftarrow$  current
23:        found  $\leftarrow$  True break
24:      end if
25:    end for
26:  end while
27:  if found then
28:    current  $\leftarrow$  goal
29:    while current is not start do
30:      subgoals.append(current)
31:      current  $\leftarrow$  current.parent
32:    end while
33:  end if
34:  return subgoals
35: end function

```

The algorithm 3 shows the pseudocode for the hybrid A* node expansion. It first iterates through all the parameterised directions (steering angles), and creates segments of the tractor's movement, forwards and backwards. All these segments are checked for feasibility, which is done by verifying if the trailer is not colliding with the tractor or with any obstacles in the environment. The feasible segments are then added to open list to be used in the next iteration of the planner and verify if a Dubins path is feasible from that new position.

In figure 3.2, the rectangle represents the tractor and the arrows the segments created, forwards and backwards, representing the recovery process. The amount of nodes, length

Algorithm 3 Expand_hybrid_node Pseudocode

```
1: function EXPAND_HYBRID_NODE(node, open_list, directions, node_length)
2:   for all sign in {-1, 1} do
3:     for all d in directions do
4:       segment  $\leftarrow$  [node.x, node.y, node.yaw]
5:       for i do in node_length
6:         new_node  $\leftarrow$  new_node()
7:         new_node.yaw  $\leftarrow$  segment.last.yaw + d
8:         new_node.x  $\leftarrow$  sign * segment.last.x + i * cos(new_node.yaw)
9:         new_node.y  $\leftarrow$  sign * segment.last.y + i * sin(new_node.yaw)
10:        new_node.parent  $\leftarrow$  segment.last.parent
11:        new_node.f  $\leftarrow$  compute_fcost(new_node, goal)
12:        segment.append(new_node)
13:      end for
14:      if check_feasibility(new_node) then
15:        open_list.append(new_node)
16:      end if
17:    end for
18:  end for
19: end function
```

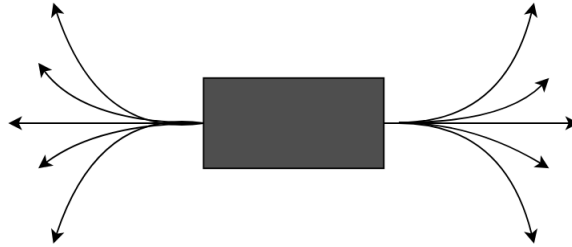


Figure 3.2: Hybrid A* node expansion.

of the segments and the maximum radius can be parameterised by the user, allowing for more diversity of operational environments.

3.3 Controller

A path is nothing if it cannot be followed so, a controller capable of attending to this system's needs is required. This controller will receive as input the generated path by the planner and will try to track it. This is achieved in two steps, first, having the current positions in mind, it will choose the next subgoal in the path. Since the controller is a PP controller, the subgoal is chosen depending on the lookahead distance, as explained in 2.3.1. The next step is to compute the angular velocity needed for the robot to reach said subgoal. For this, two controllers were used:

- **Forwards Controller:** Used when the tractor is moving forwards.

- **Backwards Controller:** Used when the tractor is moving backwards.

The choice of controller depends on the orientation of the tractor and direction to the next subgoal. The need for two controllers arises from the fact that when moving backwards, the movement needs to be optimised for the trailer's position and orientation, while when moving forwards, the movement needs only to be optimised for the tractor's movement as the trailer positions are more predictable when moving forwards.

The forwards controller is defined by the following equations:

$$\omega = \tan^{-1} \left(\frac{2 * WB * \sin(\epsilon_{\theta_0})}{l_f} \right) \quad (3.1)$$

where WB is the wheelbase of the tractor, l_f is the lookahead distance and ϵ_{θ_0} is the error in the angle between the tractor and the next goal.

$$\epsilon_{\theta_0} = \tan^{-1} \left(\frac{t_y - y_r}{t_x - x_r} \right) - \theta_0 \quad (3.2)$$

The t_x and t_y are target point coordinates and x_r and y_r are the current tractor center coordinates. As explained previously, this controller only cares about the tractor's configuration, which makes having a feasible path all the more important.

The backwards controller, on the other hand, is defined by the following equations:

$$\omega = V \left(-k(\theta_1 - \alpha^*) - \frac{\sin \theta_1}{RTT} \right) \quad (3.3)$$

where RTT is the distance between the hitch joint and the trailer's real axle, k is a constant, θ_1 is the angle between the tractor and the trailer, V is the linear velocity of the tractor and

$$\alpha^* = \tan^{-1} \left(\frac{2 * RTR * \sin(\epsilon_{\theta_1})}{l_f} \right) \quad (3.4)$$

with

$$\epsilon_{\theta_1} = \tan^{-1} \left(\frac{t_y - y_t}{t_x - x_t} \right) - \theta_t \quad (3.5)$$

where t_x and t_y are the target point coordinates and x_t and y_t are the current trailer real axle coordinates and θ_t is the orientation of the trailer. It is observed that these equations are similar to the forwards controller, however, they differ in the fact that the goal pose is defined by the trailer's position. Even though this controller is taking the trailer's constraints into account, due to the innate nature of the tractor-trailer system being non-holonomic, the path planner is still the one responsible for maintaining the feasibility of the movement.

3.4 Collision Avoidance

The collision avoidance aspect of the controller is of the utmost importance in real world scenarios when dealing with possible workers in the field. To achieve this safety requirement, the controller is equipped with a collision detection algorithm which will check for

obstacles in the way of the tractor-trailer system and remain still until the obstacle is no longer in the way or another path update has been sent.

The algorithm works by calculating the angle between the tractor and the chosen subgoal in the path, then, it will check if there are any obstacles in the rectangle created along the line connecting the tractor and subgoal. If true, the controller will signal that a collision is imminent and commands will be to stop and wait.

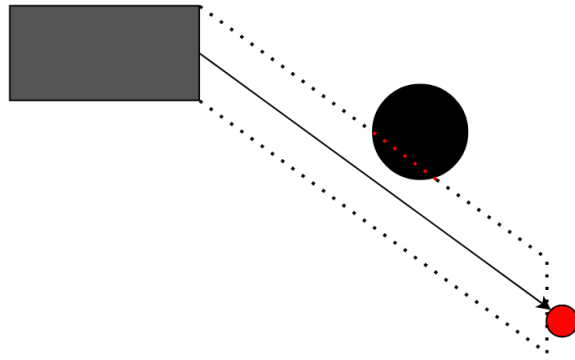


Figure 3.3: Representation of the collision detection module. In red the goal pose, in grey the tractor, the black circle is the obstacle and then the dotted rectangle the expanded rectangle used to check for collisions.

3.5 Final Architecture

The final architecture can be seen in figure 3.4, where the modules are represented and how they interact with each other. The environment is either the real world or a simulated world, and the sensors are the Lidar and wheel encoders, which can be represented by their physical counterparts or simulation plugins. The state estimation module is responsible for estimating the tractor's position and orientation using sensor data. The map used for localization must be created beforehand, for example using a mapping process. The localization module uses the map and sensor data to determine the tractor's position within the environment. Sensor data conversion modules may be required to adapt data formats, such as converting 3D point clouds to 2D laser scans. The navigation module coordinates the planning and control tasks, including path planning from start to goal positions and generating control commands for both forward and backward movements, as well as handling collision detection to ensure safe operation. The planning and control modules can be implemented using custom algorithms tailored to the specific requirements of the tractor-trailer system.

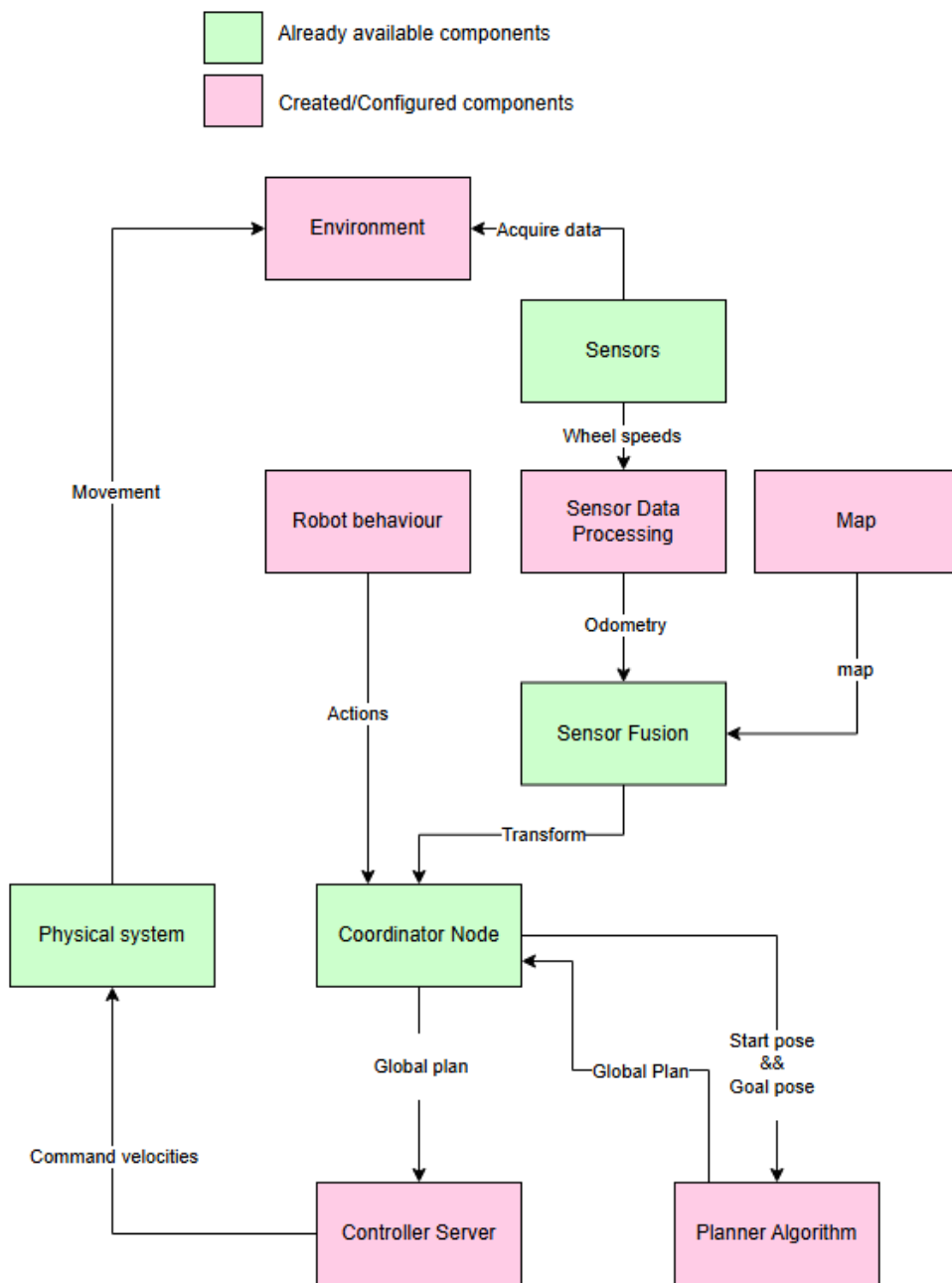


Figure 3.4: System architecture overview. In pink are the components that have been implemented or configured, and in green the already available components.

IMPLEMENTATION

In this chapter, the implementation of the different modules and components mentioned in the previous chapter will be described, as well as their process of creation and integration into the full system.

4.1 Software

Since this system is composed of several different components that need to run independently, the software used will need to be robust enough to account for each component's requirements, and for this task the [Robot Operating System \(ROS\)](#) framework is used. There are two versions of this framework, [ROS](#) and [Robot Operating System 2 \(ROS2\)](#), the latter being the most recent version, which is the one to be used in this project.

4.1.1 ROS2

The [ROS2](#) framework is a set of software libraries and tools that help developers create robotic applications. It provides a set of solutions to various problems, such as parallelism, communication, modularity, and hardware abstraction.

It works by creating a network of nodes (python or c++ programs) that can communicate with each other using a publish-subscribe model and a service-client model. The former is a broadcasting model where a node can publish messages to a specific topic, and any other program can subscribe to that same topic and receive those messages and use them using callbacks. The latter is a request-response model where a specific node is the server and other nodes can call it to request a specific service, which helps with modularity as each node can have its own specific task and be developed independently. When it comes to the hardware abstraction, since the software is wildly used in the robotics community it already has a lot of packages and libraries that can be used to interpret data from sensors, control actuators, and even simulate the robot in a virtual environment.

4.1.2 NAV2

The [Navigation 2 \(NAV2\)](#) stack is a set of packages that provide a framework for autonomous navigation. It is built on top of [ROS2](#) and provides a set of tools for coordinating the different components of the navigation system.

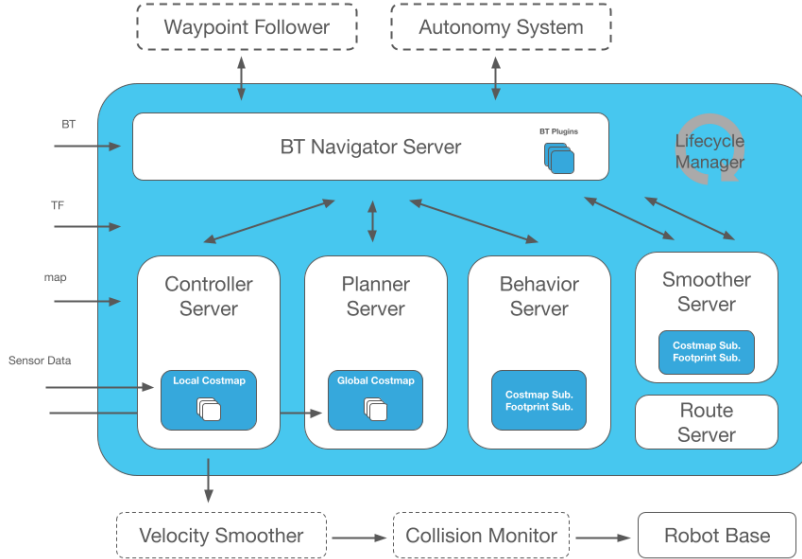


Figure 4.1: NAV2 stack architecture [49]

In figure 4.1 we can see the different components of the [NAV2](#) stack as well as their relations with one another. Firstly, let's define the inputs to the diagram. The BT is the Behaviour tree which is an xml file that defines the robot's behaviour, the TF a collection of transforms that define each robot link to one another, the map is a 2D map representing the environment, and the sensor data is the data collected by the robot's sensors. Secondly, some essential elements are also the global and local costmaps, which are 2D maps that instead of having binary values for if there's an obstacle or not, have costs for each cell that represent the difficulty of traversing that cell, the Global costmap has the map origin as a reference for the robot's position, while the local costmap is centered around the robot's position. Having these concepts defined, we can now explain the different components of the [NAV2](#) stack. The BT navigator server is the main component of the navigation as it manages and interacts with all the other servers to achieve a robust navigation solution. The Controller server, given the global path and the local costmap, is responsible for generating velocity commands for the robot to follow the path, it does this by using a controller plugin that can be custom made or one of the many already available in the stack. The Planner server is responsible for, given the global costmap and the robot's position, generating a global path to the goal, it does this by also using a plugin. The Behaviour server is given both costmaps and decides what action the robot should take in a given moment. Lastly, the Lifecycle manager, this node is responsible for managing the lifecycle of all the other nodes in the navigation stack, ensuring that they are properly initialized, configured, and shut down as needed. These are the main components as the

other servers are not essential for understanding the navigation and overall architecture of the system.

4.2 Hardware

The tractor used is an Agilex Scout which is a four wheeled differential driven robot, equipped with a NVIDIA Jetson Agx Xavier as the main computer, a LIDAR and wheel decoders. the NVIDIA Jetson Agx Xavier is a powerful computer capable of running complex algorithms in real time, and is used to run the whole system, from path planning to control and sensor perception. The Lidar and encoders are used to gather data for localization and mapping. This robot can be teleoperated using a controller, or can be programmed to do whatever autonomous task is required since all its instruments are accessible in the Jetson Agx Xavier. The tractor is shown in the figure below:



Figure 4.2: Simulated tractor in Gazebo.

There's no representation of the jetson in the simulation since the program is running on the same machine as the simulation. However, it is possible to notice the Lidar rack on top of the other instruments. Once again, this is but a representation for simulation purposes, as the real tractor has a similar configuration, shown in figure 4.3.

The figures 4.3 and 4.4 show the robot, its dimensions, and also the additional rack, at the top, where the computer, Lidar and all other required electronics are mounted.

Additionally, the tractor is pulling a trailer, which is equipped with a spray system, however for the sake of simplicity, to test the navigation and control algorithms, the tests were done with the following trailer:



Figure 4.3: Real tractor.

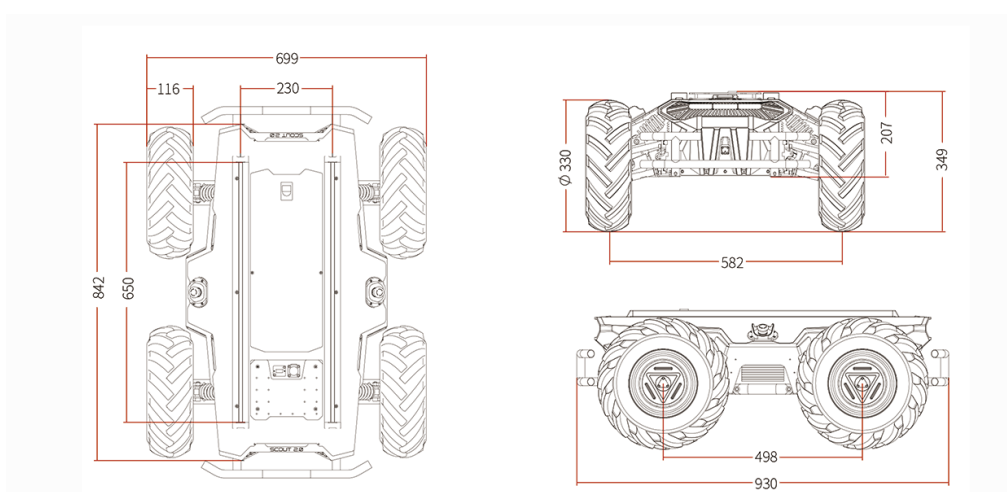


Figure 4.4: Agilex Scout dimensions [50].

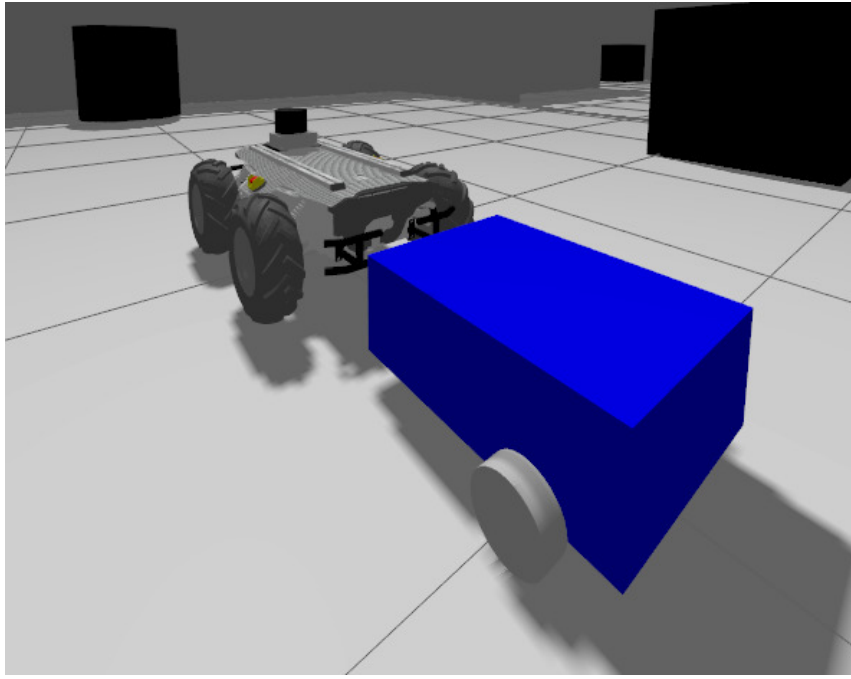


Figure 4.5: Tractor-trailer system simulated in Gazebo Classic.

The trailer shown in figure 4.5, is a representation of a generic trailer, not having any specific functions other than following the systems dynamics, which is the main focus of this work. One particular aspect of this robot is that there's no sensor for trailer position and, therefore, it is estimated in real time using the system's dynamics shown in 2.5.1.

4.3 Environment

For development purposes, a virtual environment is used to develop the navigation software and test it without the need for a physical robot. This environment can be created using Gazebo, a robotics simulator that is compatible with ROS2, and it allows the user to create a world in xml format, specifying the different physical properties of the environment as well as the structures and objects inside it.

Since the robot will be operating in an agricultural environment, the world created for the simulation would have to reflect that, so a simple world was created with five corridors with traffic barriers on each side (to simulate trees or crops) and some additional obstacles to make for a more complex environment.

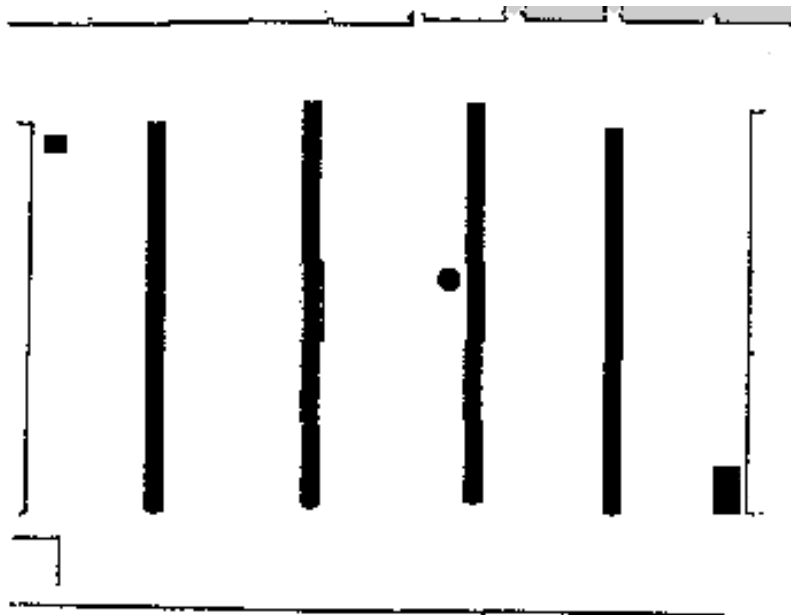


Figure 4.7: Map created using the SLAM Package in the Gazebo Simulation. White space is non-occupied space, black are obstacles and grey is undiscovered space.

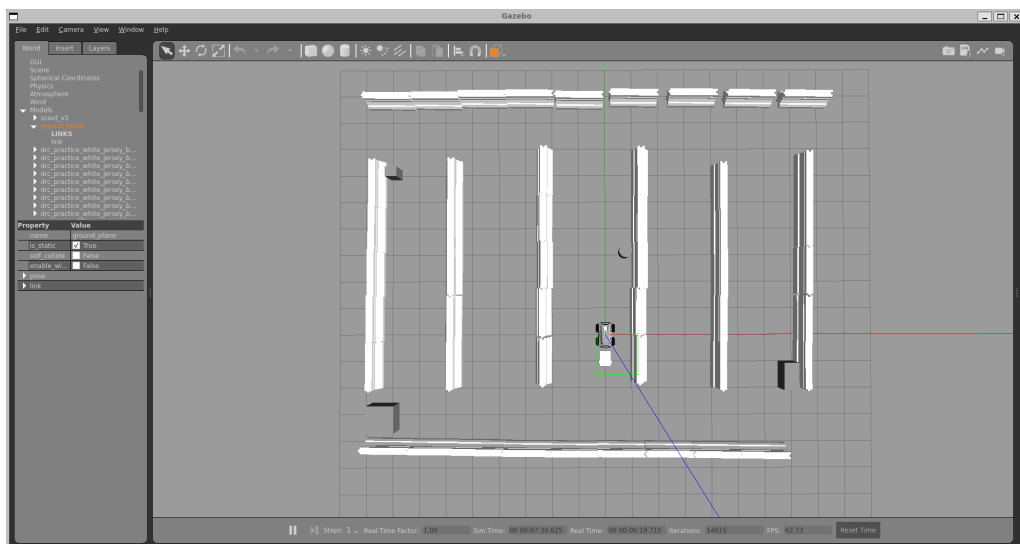


Figure 4.6: Gazebo world used for simulation.

Having the world isn't enough to have a fully autonomous robot, a map of the world is also required for the localization and navigation components to work. this map can be created using the [SLAM](#) algorithm, as mentioned in the previous chapter [2.4.2](#). Since the [NAV2](#) stack already has a package that implements the [SLAM](#) algorithm, all it needs is to have the robot's model and sensors running in the environment, and it will create a map. The robot model used in this work is fortunately made available by its manufacturers so it can be used in the simulation directly, and the sensors are simulated using their Gazebo plugins, which allow the user to specify the sensor's properties, such as range, resolution, and noise.

The map shown in figure 4.7 is the result of mapping the simulated environment, however, since this work aims to have an operational prototype, two other maps were created in real world locations, one in a concealed room and another in a corridor with a few obstacles to simulate the rows of crops.

These last two maps, due to being created in real world locations, can't be simulated in gazebo, so the hardware interface for the robot and its sensors would need to be implemented in order to communicate within the [ROS2](#) framework. Fortunately the necessary packages were all provided by the manufacturers [51, 52] and only needed a few adjustments to be completely integrated within the system. Since the LIDAR used is a 3D LIDAR, the output of the sensor is a point cloud, however, the [SLAM](#) package used outputs 2D Maps and would need a Laser Scan to be used. To overcome this a [ROS2](#) package was used (Pointcloud to Laser Scan) that given the distance and angles that need to be covered, converts a point cloud into a laser scan, allowing for the [SLAM](#) package to work as intended.

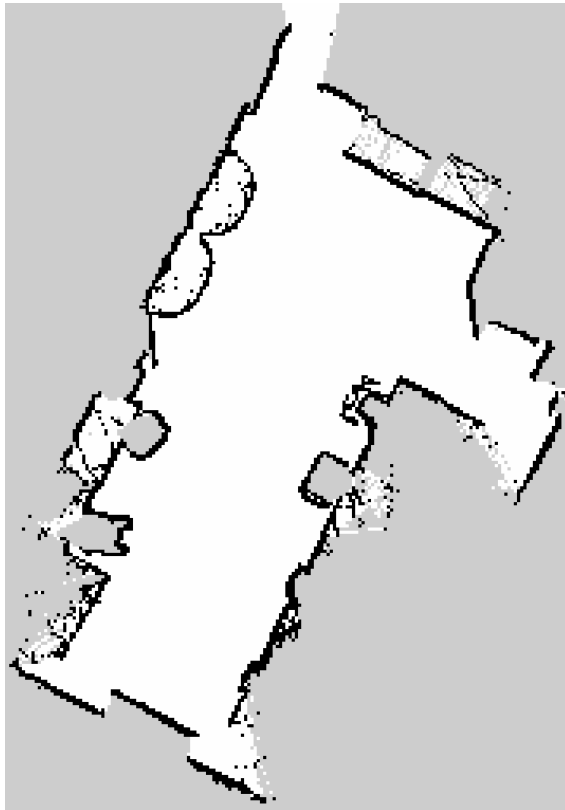


Figure 4.8: Map of the concealed room.

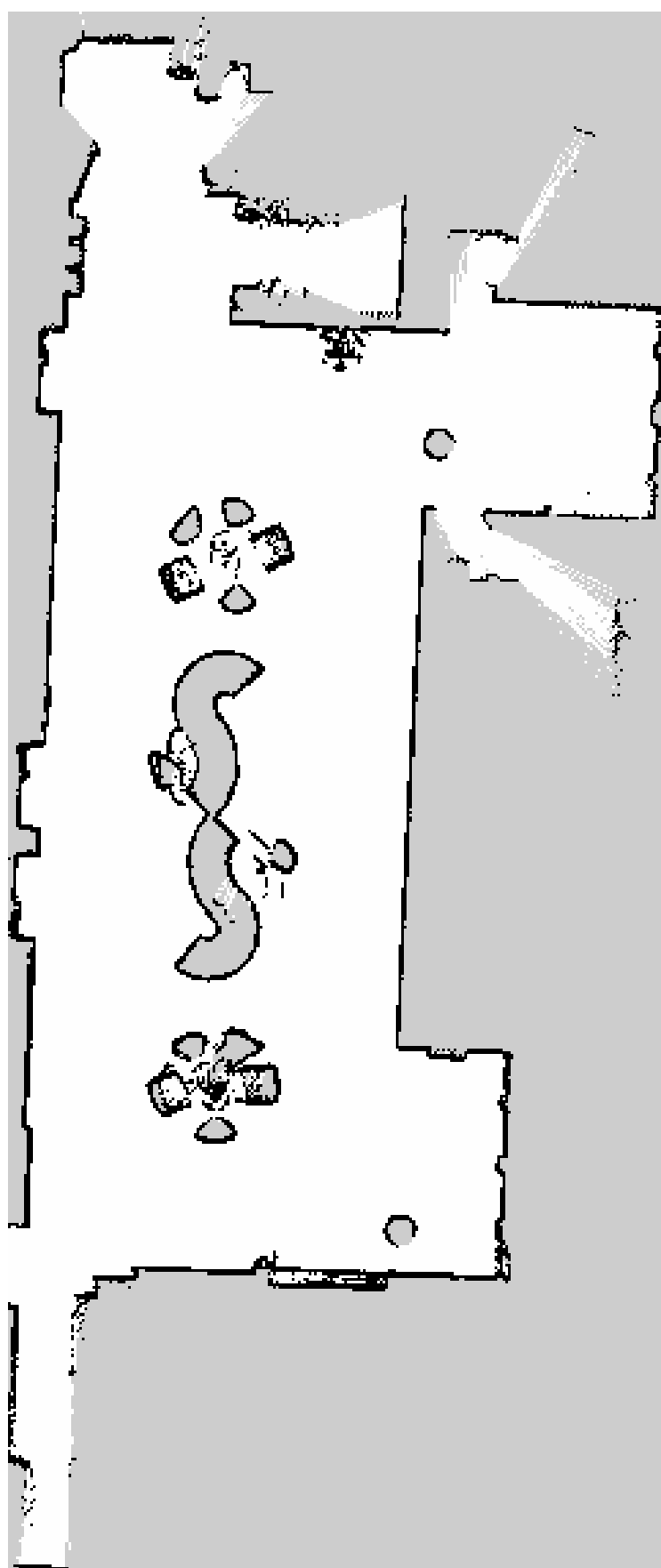


Figure 4.9: Map of the corridor.

To visualize the robot in these maps as well as all the different data that is deemed relevant, a software called Rviz2 is used. This software allows the user to select the various ROS2 topics that are being published by the running nodes and visualize them in a 3D environment, which is very useful for debugging and testing purposes.

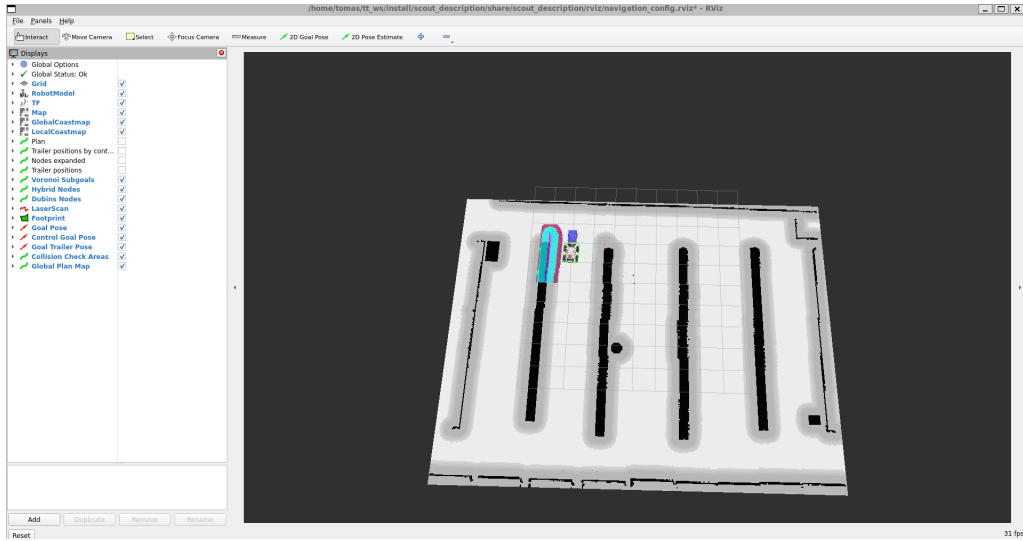


Figure 4.10: Rviz2 visualization of the robot in the simulated environment.

The figure 4.10 shows, at the left, the different data provided by the developed system and, above it the navigation tools like estimatin the robot's initial position and goal generation. These last two tools can be used manually in Rviz2 or be published by a custom node if the user requires it.

4.4 Planning algorithm

As explained in the previous chapter 3.2, the planner is devided into three main components, the Voronoi Graph, the Dubins Path and the Hybrid A* recovery algorithm.

4.4.1 Voronoi Graph

The main function of the Voronoi Graph is to create a set of points in space that can be searched for a simple path to the goal using an A* search. Due to the nature of calculating a Voronoi Graph, it can be very computationally expensive, so the algorithm is ran offline, when the environment is mapped, and the resulting graph is saved to a file for the online planner to use. To create this graph, a Ros2 python node was created that executes a script with the previous behaviour.

The algorithm first works by creating black and white image containing the edges of the obstacles and grouping them into a single column of points which are then used to calculate the Voronoi Graph using the Scipy library [53]. This graph is then filtered to remove points that are inside the obstacles and remove points that are too close to each

other. Points can be created inside the obstacles because of their width, so the algorithm considers it available space. To filter them, they are place on the original map, and if they're not in white space, they're removed.

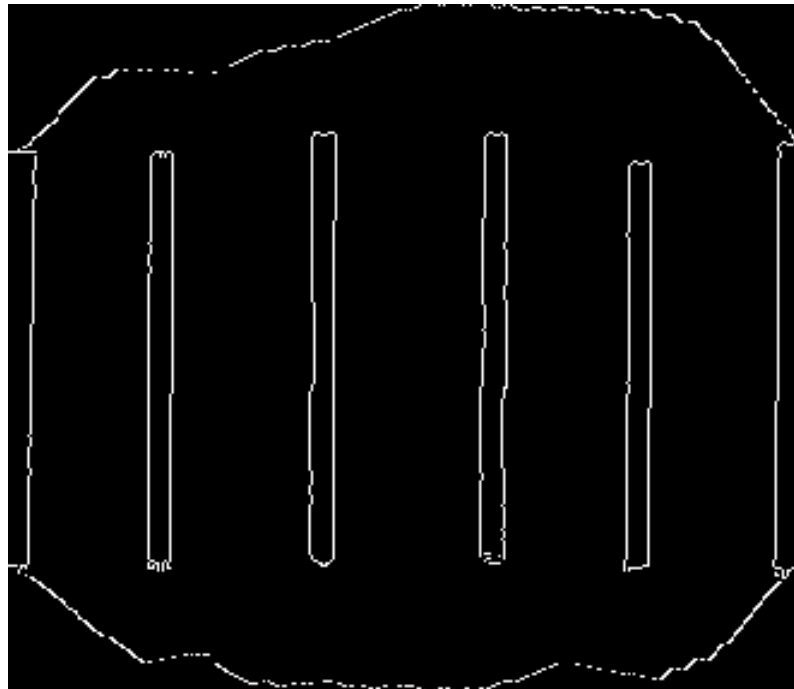


Figure 4.11: Image with the obstacle edges.

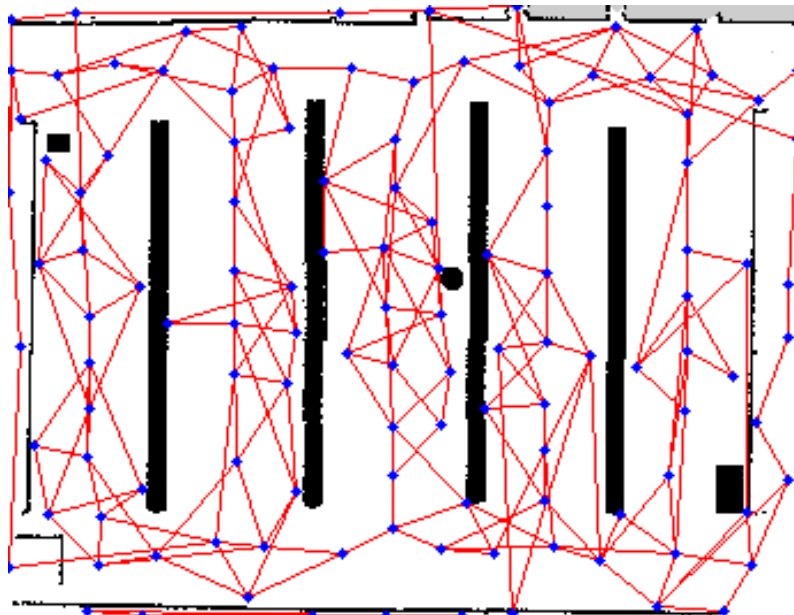


Figure 4.12: First Voronoi Graph created for the environment in figure 4.6.

It is possible to verify that the graph isn't exactly perfect, as it doesn't show the usual behaviour of a Voronoi Graph with straight lines equidistant to the obstacles, however, this is due to the jagged nature of the edges of the obstacles, creating several equidistant

points. Despite this, this graph is poorly dense in some areas compared to others, so a second iteration is made to correct this.

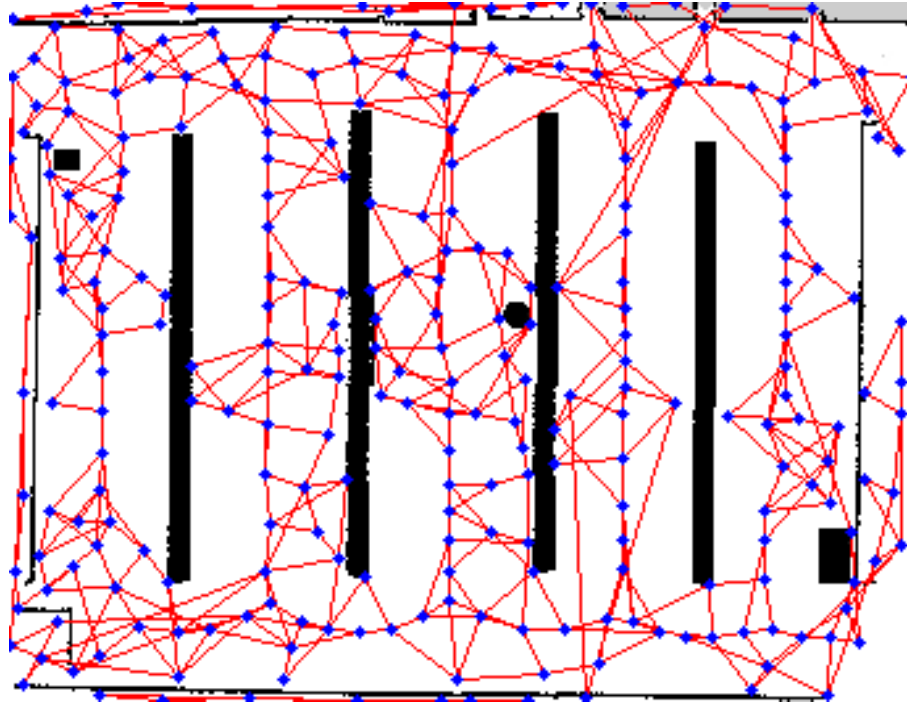


Figure 4.13: Second Voronoi Graph created for the environment in figure 4.6.

And then finalized with a third iteration that now resembles a more traditional Voronoi Graph.

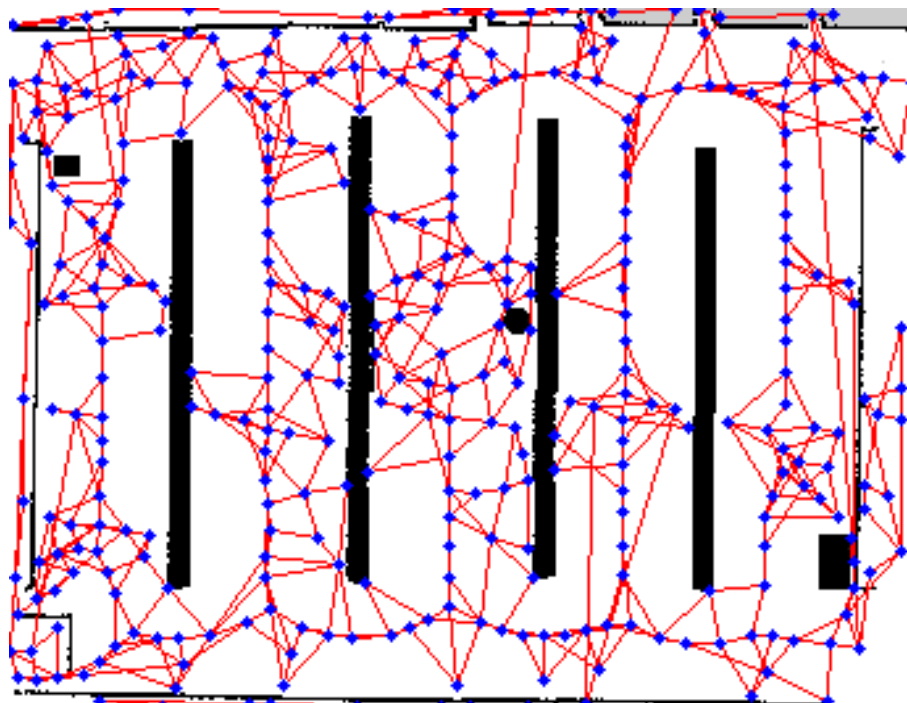


Figure 4.14: Final Voronoi Graph created for the environment in figure 4.6.

It is now possible to verify the straight segments between the obstacles in the less obstacle dense areas, which allows for more efficient path planning. The denser areas having more nodes and edges allows for more pathing options which is useful for obstacle avoidance. The nodes and edges are then saved to a file to be then used by the planner.

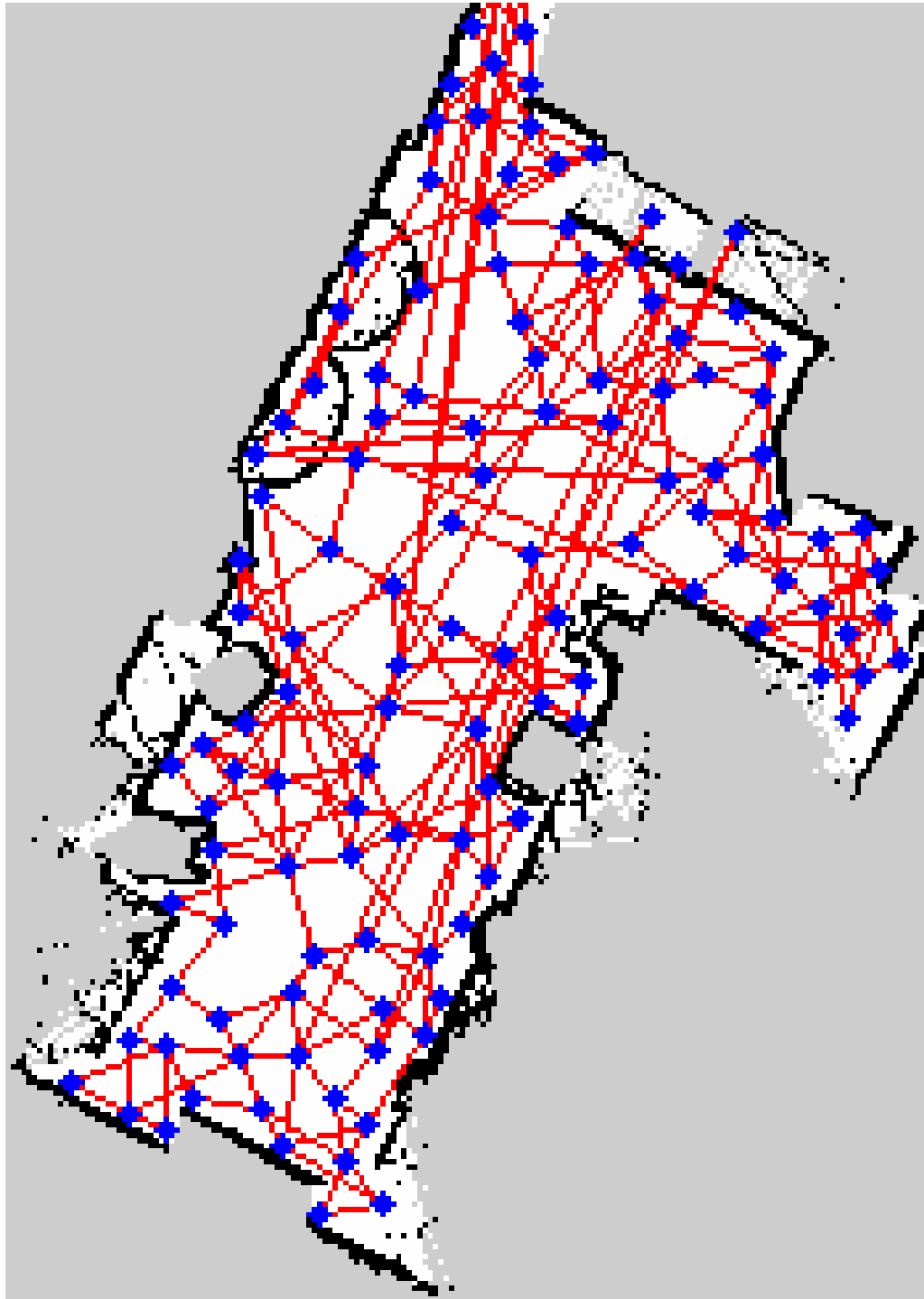


Figure 4.15: Concealed room Graph.

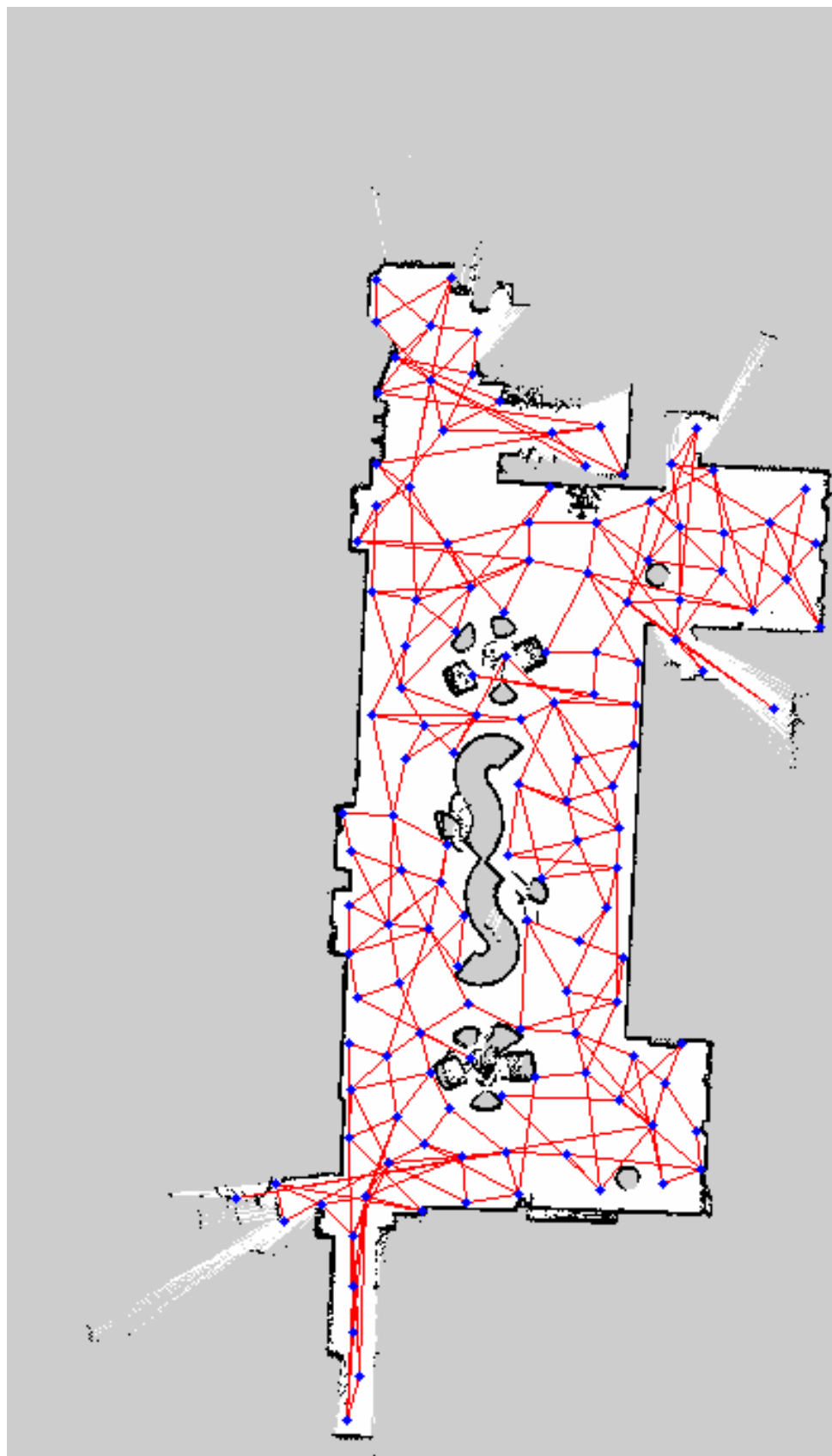


Figure 4.16: Corridor Graph.

Once again, the Voronoi Graphs aren't the usual straight line ones however, the environments used are not simple and have several obstacles leading to irregular graphs.

4.4.2 Planner Plugin

As mentioned in the subsection 4.1.2, the [NAV2](#) stack allows for the creation of custom plugins that are used by the different servers to perform their tasks. In this case, a custom planner plugin was created to be used in the Planner server, responsible for creating a global plan for the robot to follow. This plugin is written in C++ and uses the [NAV2](#) plugin interface to be recognized by the BT Navigator server.

The plugin is responsible for the Dubins Path and Hybrid A* recovery algorithm, as well as the A* search algorithm that is used to find the path between the start and goal points. It is done by reading the file with the Voronoi Graph, verifying the closest nodes to the start and goal points, and then searching for the path. The resulting subpath is shown in figure 4.17 visualized in Rviz2. The reason this path cannot be used directly is because it is not a continuous smooth path, it is a set of points that serve as heuristic for the planner and some points could be connected in ways that are not feasible for the robot, such as reversing, and, therefore, a Dubins Path needs to be created.

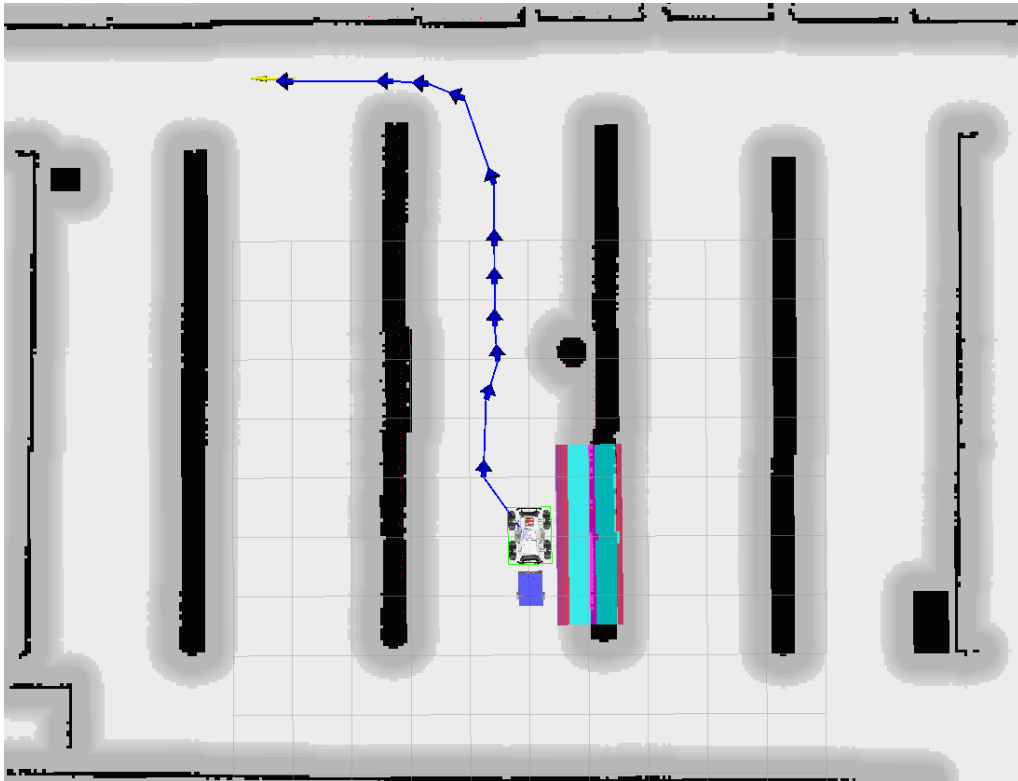


Figure 4.17: Subpath, in blue, created by the planner.

A feature of the planner is the addition of the trailer. The planner needs to take into account the position of the trailer to ensure that no collisions occur while the robot is following the path. However, the [NAV2](#) stack has a limitation. There's a package within

the stack that allows for the calculation of the robot's joint values, the joint state publisher. This package takes in the robot's model, described in a [Unified Robot Description Format \(URDF\)](#) file, and calculates the joint values based on the robot's movement. However this package does not account for passive revolute joints, like the trailer connector or trailer hitch. Not accounting for this would mean that the trailer would either not be considered, which wouldn't make sense as it is the whole purpose of this robot, that the trailer would be considered fixed to a certain position, however this solution would not be feasible as it might make some curves impossible to follow, so a custom publisher was made to publish the trailer's hitch transform based on the trailer's movement. This publisher takes in the robot's dynamics defined in [2.5.2](#) and integrates the tractor's movement allowing for approximate estimation of the trailer's hitch position and orientation.

Having the trailer estimated and a rough path to follow, the next step is to create the Dubins path to the desired subgoal. As explained in [3.2](#), starting from the farthest subgoal, a Dubins path is created from the tractor's current position to the subgoal. Naturally, since a Dubins path is a collection of two curves and a straight line, the path created may not be feasible as it might go over obstacles or even put the trailer in undesirable positions. To check for this, with every iteration of the planner, the trailer position is estimated in every point of the current plan and a verification against jackknife conditions and obstacle collisions is performed. If any of these conditions are met, the Dubins path is void and a path to the next subgoal is created.

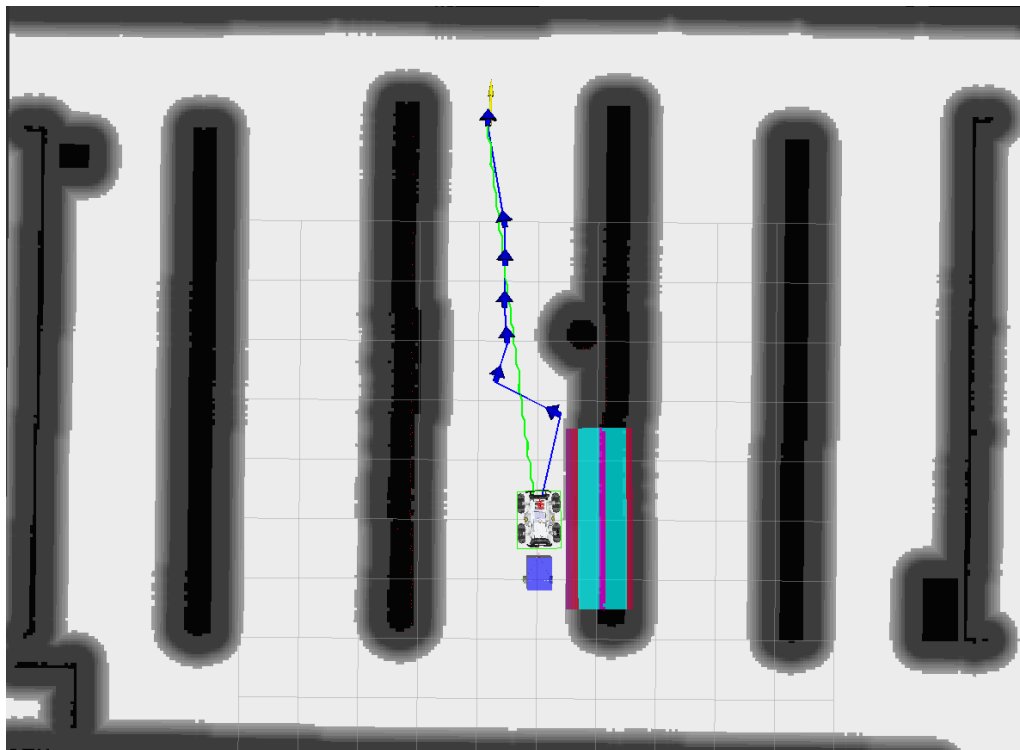


Figure 4.18: Dubins Path created by the planner in the first iteration.

In picture [4.18](#), it is possible to see how the planner chooses the farthest node and tries

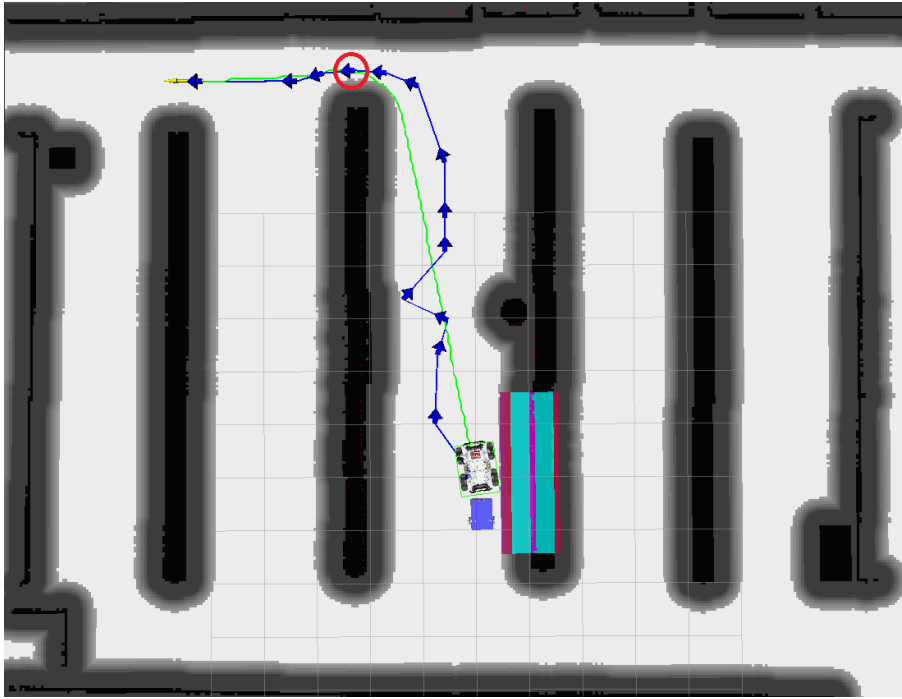


Figure 4.19: Dubins Path created by the planner in three tries. The red circle marks the subgoal used as intermediary.

to connect it to the starting position, and, since there are no obstacles or movements that would make the trailer jackknife, the Dubins path is valid and used. However, in picture 4.19, the planner tries to connect the tractor to the last subgoal, but cannot due to the row of crops in between making the planner retry three times before a suitable subgoal is found and, because the chosen subgoal is in clear view and aligned with the goal position, when the planner goes to repeat the algorithm and a direct path is found.

The last step to finish the controller is developing the recovery hybrid A* component. The previous examples showed how iterating through the subgoals can lead to a valid path, however, in certain cases it may not be the case and the loop would reach the start point without a valid path.

For these cases, a especially designed recovery module is implemented. It works by, first, reading the configuration file to look for the maximum angles the arcs should have. Then, it devides the maximum angle by the number of arcs the algorithm should have, forwards and backwards. These arcs are composed of a user defined number of points distanced by a user defined distance, which the last point will be used as a new starting point and iterate through the subgoals again.

The process of creating these arcs uses the same logic as the verification of the Dubins path for jackknifing, but instead of checking only for the trailer's hitch position, it checks for the tractor's position and orientation aswell. It is a loop iterated over the number of points starting form the starting position and goes one by one, calculating the next point as if the trailer was steered through the defined angle. This process created a number of arcs each time and can get computationally expensive if no subgoal can be reached over a

prolonged period of time. To mitigate this, a time limit is imposed and the user will have to manually intervene to adjust the robot or simply set a new goal and try again.

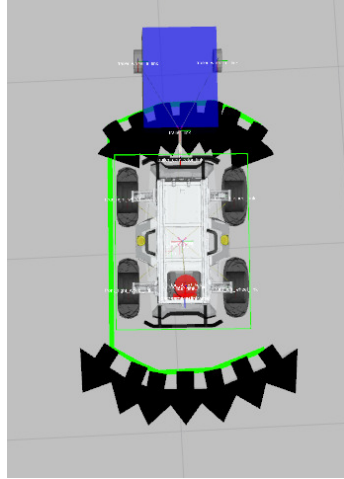


Figure 4.20: Hybrid A* arcs.

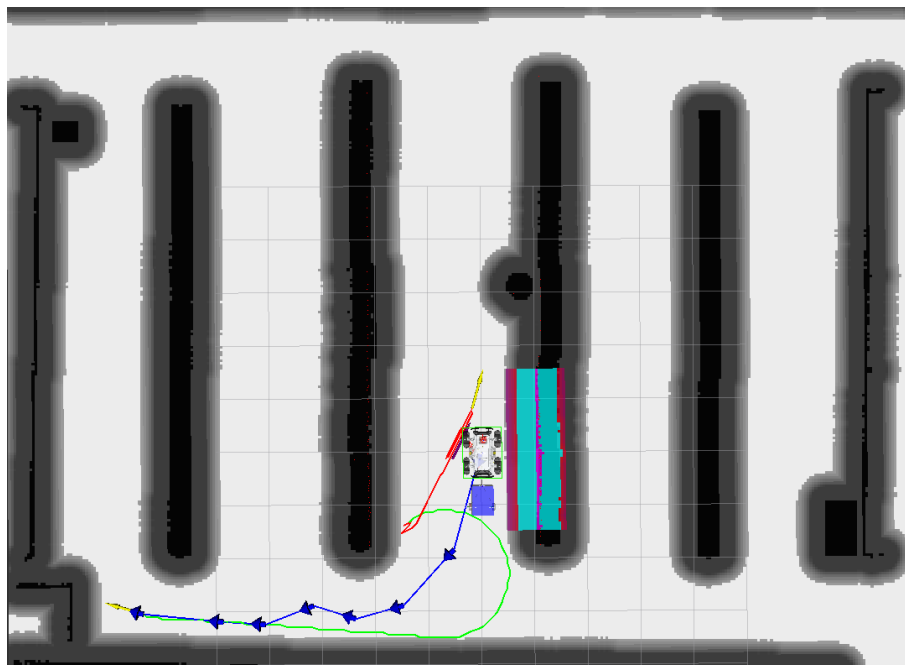


Figure 4.21: Successful recovery path with number of segments as one. Hybrid A* path in red, Dubins path in green, and subgoals in blue.

At first, the number of segments was not a variable and the algorithm would always add one point for every iteration of the hybrid A* algorithm. This would not only worsen the computation time but also lead to very small adjustments in paths which could make them unfollowable by the controller, as shown in Figure 4.21.

This, of course, led to the need for the number of segments, and their length, to be a variable parameter and the problem was solved. The figure 4.22 shows an attempt at making a ninety degree turn backwards. Since the Dubins path can only find paths

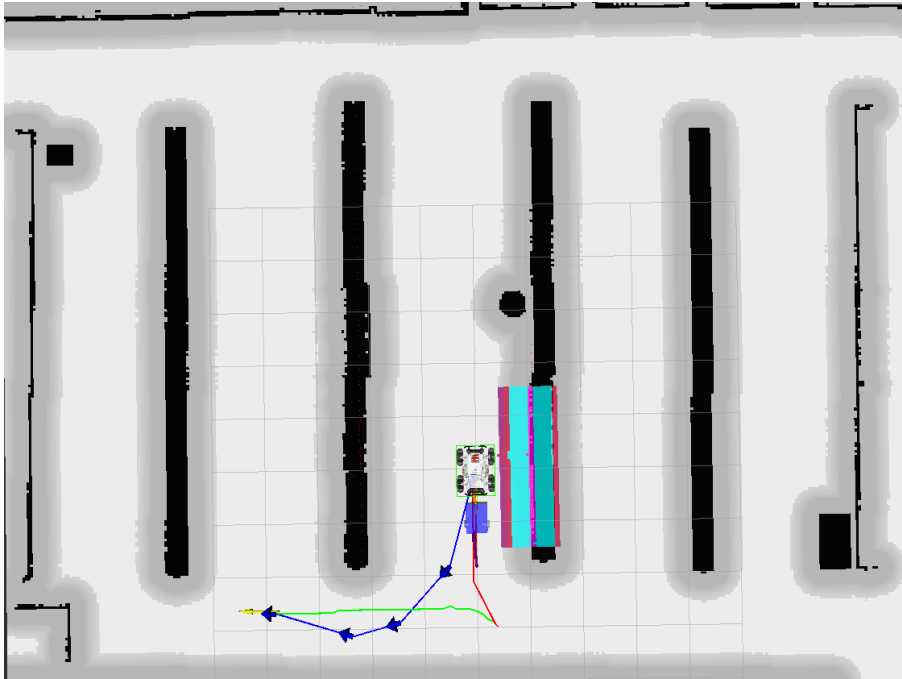


Figure 4.22: Successful recovery path with number of segments as fifteen. Hybrid A* path in red, Dubins path in green, and subgoals in blue.

that make the robot move forwards, the hybrid A* was called and made the necessary segments to allow for the manoeuvre to be completed successfully.

The conventional A* has the following cost function for each node:

$$f(n) = g(n) + h(n)$$

where $f(n)$ is the total cost of the node n , $g(n)$ is the cost to reach the node from the start node, and $h(n)$ is the heuristic cost to reach the goal node from the current node. However, in this case, since the orientation is a very important factor, it must be factored into the cost of each node, so the cost function is modified to:

$$f(n) = g(n) + h(n) + ap(n) + dir(n)$$

where $ap(n)$ is the angle penalty relative to the goal pose, and the $dir(n)$ is the direction change cost. In an initial phase the robot would be constantly making changes in direction going forwards and backwards multiple times, so the direction change cost had to be implemented to avoid unnecessary oscillations and facilitate the controller's job of following the planned path.

These changes would not be enough in the end to make for efficient short hybrid path recoveries, and the last change made was to make the $h(n)$ cost incremental, making the cost of long segments too heavy to be chosen as the next node, and conditioning the algorithm to prefer shorter paths. The final expression was the following:

$$f(n) = g(n) + h(n) + h(n - 1) + ap(n) + dir(n)$$

4.5 Controller Plugin

The controller plugin is the component responsible for giving accurate velocity commands for the robot to follow the planned path. In the NAV2 stack, to the velocity commands have a specific type and there's only the need to change the linear and angular attributes of the message and return it. The controller's implementation, as a plugin, is similar to the planner's in the sense that it is a C++ class that implements the controller interface that has only a few methods that need to be implemented. The first method is the setPlan method. As the name suggests, this method receives the global plan created by the planner and stores it for when the controller may be called to produce velocity values. Since this controller, when in reverse, uses the trailer as the origin of movement, it would not make sense to have the tractor's plan as the goal position, therefore, when the setPlan method is called, the global plan is stored as well as a second plan with the trailer's position for each tractor position.

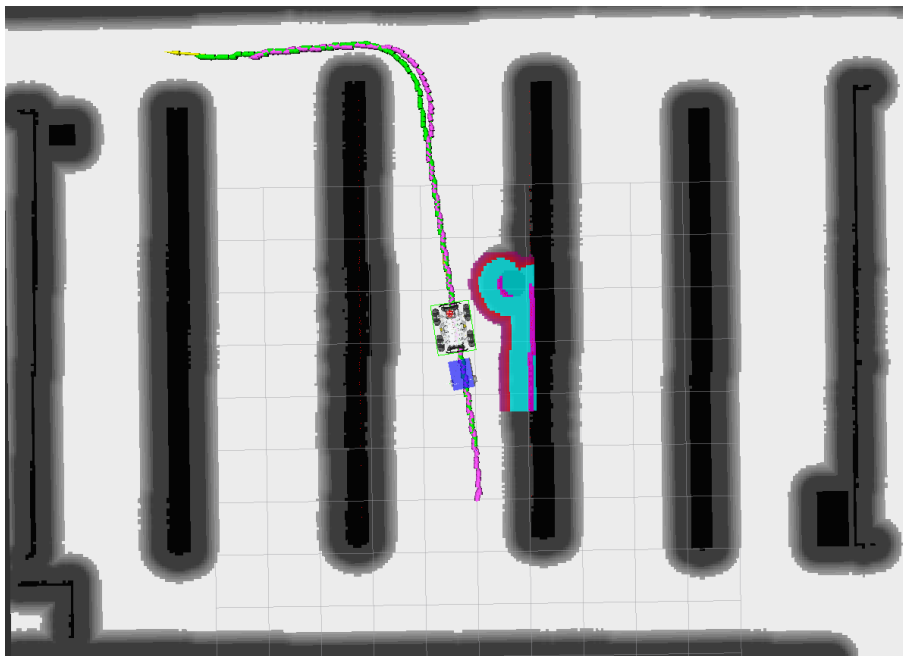


Figure 4.23: Trailer's positions in pink. Tractor's positions in green.

It is possible to observe in figure 4.23 that the trailer's positions are not the same as the tractor's and curve in a different manner, as the trailer would.

The next method is the computeVelocityCommands method. This method receives the current robot pose and computes the velocity values for the robot to have the desired behaviour for its task. Since the used controller is the pure pursuit controller, the first step is to compute the lookahead point in the stored path. For this, a for loop is used, starting from the last point used, zero if it is the first time the controller is called, and iterating over the points in the path until the lookahead distance is reached and the point chosen. If the line between the current position and the point has an angle difference of more than ninety degrees with the current robot heading, the robot will assume a reverse

movement and instead of using the global path's point, the trailer's path point in the same vector position is used. Finally, with a constant linear velocity, changing only the sign for reversing or forwards movement, the angular velocity is calculated using the expressions from section 3.3, where the only adjustment made was to set the $k = 2$. This value was chosen after some testing and it was found to be the best value for the controller to follow the path while ensuring that the trailer doesn't jackknife.

The collision detection was also implemented in the controller plugin as all that is needed for the robot to stop is to set both angular and linear velocities to zero. The implementation was straightforward, as explained in section 3.4, with the only caveat being that since the controller is using the local costmap for positioning, there was the need to create auxiliary methods to get the transform the local position to the global position, that is referencing the map's origin.

4.6 Behaviour Tree

The original behaviour tree used by the robot calls for a plan once per second. This is to ensure that the plan is always up to date with any changes in the environment and to correct any navigation errors that may occur. However, due to the nature of the tractor-trailer system, it was found that this was too frequently, as the new calculated paths would cause the tractor to change directions abruptly, which would lead to unwanted movement by the trailer. To account for this, the frequency of the planner was changed to run once every twenty seconds, which ensured that the tractor would follow the initial path and only change it if it gets in a situation where no progress is being made.

TESTS AND RESULTS

There are two main types of tests that can be performed on the navigation system. The first is the path tracking, where the processing time and the time to the goal pose are measured. The second is the collision detection to evaluate how safe people or structures are near the robot. Since the navigation system has integrated noise and uncertainty, the test results may vary, especially in the real world scenarios where the starting and goal poses can be slightly different leading to extremely different results.

5.1 Path Tracking Tests

The conducted tests aimed to evaluate how fast the algorithm can generate a path and if the robot can reach the goal pose by tracking the generated path. The first test is a direct path, where the goal is posted in front of the robot. The second is a curved path, where the goal is posted behind an obstacle but the robot can reach it going forwards. The third and last is a recovery test, where the goal is placed to the side of the robot, forcing it to go backwards to realign itself. Every test is ran both in a simulation and in the corridor environment. The simulated tests were made in a 13th Gen Intel(R) Core(TM) i9-13900H (2.60 GHz), 32 Gb RAM, NVIDIA GeForce RTX 4070 with 12 Gb of VRAM, laptop running Ubuntu 22.04 in wsl2. Every test is conducted with 0.8 meters of lookahead distance, 0.3 m/s maximum linear speed and 0.5 m/s maximum angular speed as the controller parameters, and, a turning radius of 1.2 meters, 15 hybrid segments of 10 centimeters each as the planner parameters. Since the simulated environment is different from the real world scenarios, these tests are not a comparison between the two, but rather a way to evaluate the performance of the navigation system in different conditions. The test goes as follows, first the robot's pose is estimated, this is done by selecting the position where the robot is located in RVIZ or by launching the navigation stack with the position in the parameters. The latter can only be done in simulation due to the certainty of the location where the robot is initialised. It is expected that in the real world tests the initial poses estimation will be less accurate which will lead to different trajectories even with the same goal pose.

5.1.1 Direct Path

5.1.1.1 Simulation Results

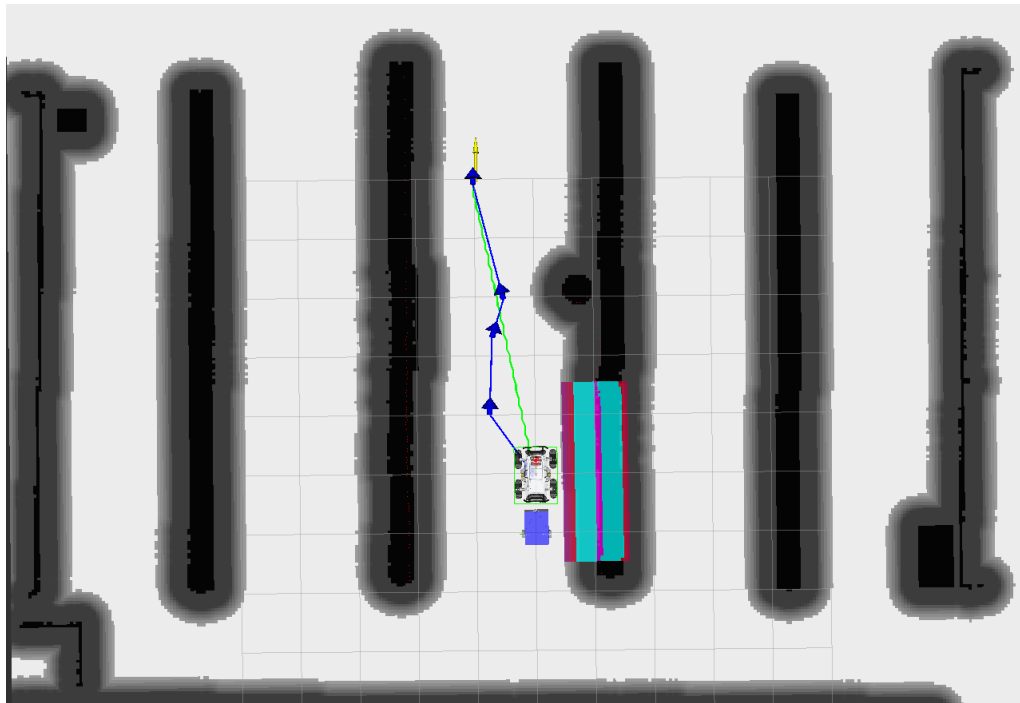


Figure 5.1: Direct path test setup in the simulated environment. Goal pose in yellow.

After five repetitions these were the results obtained in the simulation:

Table 5.1: Simulation direct path creation results.

Test	Processing Time (ms)	Dubins Length (m)
1	16.61	5.23
2	15.65	5.23
3	14.87	5.23
4	16.02	5.23
5	16.41	5.23
Mean	15.91	5.23
Standard Deviation	0.69	0

Table 5.2: Simulation direct path tracking results.

Test	Time to goal (s)	Total Length (m)
1	20.06	5.23
2	19.87	5.23
3	19.54	5.23
4	20.11	5.23
5	19.72	5.23
Mean	19.86	5.23
Standard Deviation	0.24	0

5.1.1.2 Real World Results



Figure 5.2: Direct path test setup in the corridor. Goal pose in yellow.

After five repetitions these were the results obtained in the corridor:

Table 5.3: Real world direct path creation results.

Test	Processing Time (ms)	Dubins Length (m)
1	64.01	8.88
2	67.48	8.89
3	55.63	8.83
4	55.86	8.88
5	52.74	8.87
Mean	59.14	8.87
Standard Deviation	6.27	0.02

Table 5.4: Real world direct path tracking results.

Test	Time to goal (s)	Total Length (m)
1	37.92	8.88
2	37.13	8.89
3	38.03	8.83
4	38.19	8.88
5	38.32	8.87
Mean	37.92	8.87
Standard Deviation	0.47	0.02

5.1.2 Obstructed Path

5.1.2.1 Simulation Results

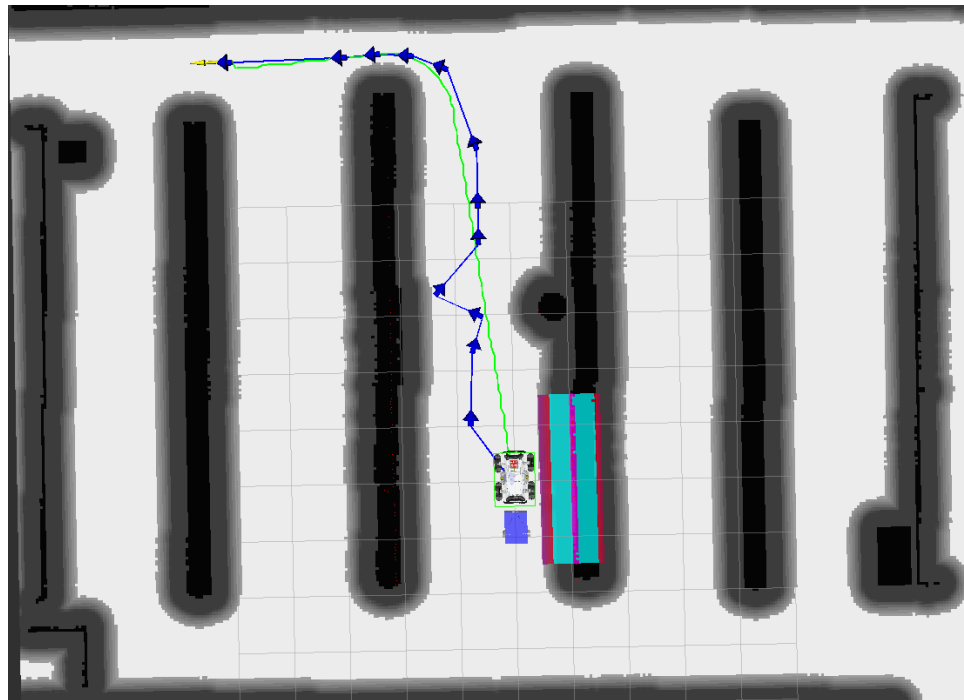


Figure 5.3: Obstructed path test setup in the simulated environment. Goal pose in yellow.

After five repetitions these were the results obtained in the simulation:

Table 5.5: Simulation obstructed path creation results.

Test	Processing Time (ms)	Dubins Length (m)
1	20.84	11.38
2	17.90	11.38
3	18.05	11.38
4	18.62	11.38
5	18.43	11.38
Mean	18.77	11.38
Standard Deviation	1.19	0

Table 5.6: Simulation obstructed path tracking results.

Test	Time to goal (s)	Total Length (m)
1	51.83	11.38
2	50.52	11.38
3	51.45	11.38
4	53.70	11.38
5	52.44	11.38
Mean	51.99	11.38
Standard Deviation	1.18	0

5.1.2.2 Real World Results



Figure 5.4: Obstructed path test setup in the corridor. Goal pose in yellow.

After five repetitions these were the results obtained in the corridor:

Table 5.7: Real world obstructed path creation results.

Test	Processing Time (ms)	Dubins Length (m)
1	57.43	11.89
2	56.71	11.87
3	56.72	11.88
4	66.03	11.91
5	66.50	11.89
Mean	60.59	11.89
Standard Deviation	5.11	0.01

Table 5.8: Real world obstructed path tracking results.

Test	Time to goal (s)	Total Length (m)
1	51.83	11.88
2	50.52	11.87
3	51.45	11.88
4	53.70	11.91
5	52.44	11.89
Mean	51.99	11.89
Standard Deviation	1.18	0.02

5.1.3 Recovery test

5.1.3.1 Simulation Results

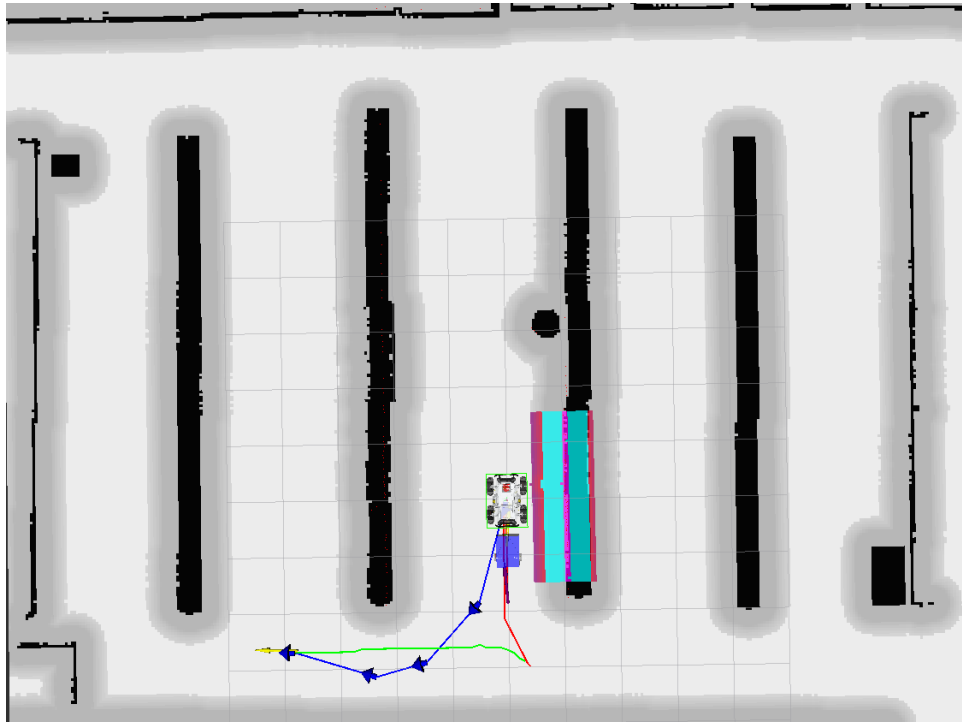


Figure 5.5: Recovery test setup in the simulated environment. Goal pose in yellow.

After five repetitions these were the results obtained in the simulation:

Table 5.9: Simulation recovery creation results.

Test	Processing Time (ms)	Dubins Length (m)	Hybrid A* length (m)
1	25.99	6.10	4.53
2	25.51	6.10	4.53
3	22.84	6.10	4.53
4	23.81	6.10	4.53
5	22.91	6.10	4.53
Mean	24.21	6.10	4.53
Standard Deviation	1.47	0	0

Table 5.10: Simulation recovery tracking results.

Test	Time to goal (s)	Total Length (m)
1	20.83	10.63
2	20.61	10.63
3	21.14	10.63
4	20.89	10.63
5	20.45	10.63
Mean	20.78	10.63
Standard Deviation	0.27	0

5.1.3.2 Real World Results

In the real world, the recovery test was not very reliable as the recovery process varied significantly between trial, however the conducted trials had the following results.



Figure 5.6: Recovery test setup in the real world environment. Goal pose in yellow.

It is possible to verify that the robot, despite being in a similar initial pose and trying to achieve a similar goal pose, the planned paths are significantly different, like in figure 5.7, which can sometimes lead to the robot not being able to reach due to the path having a large amount of recovery turns demonstrated in figure 5.8. However, since the behaviour tree is designed to have the planner run every 20 seconds, the planner is sometime able to find a more desirable solution while still tracking the first plan. This often corrects the initial trajectory, leading to a smoother path. This behaviour was present during the third test as it began as a more complex recovery path, but after a few seconds the planner found the path in figure 5.9.

Naturally, due to having different paths, the processing times and lengths of the paths are also different as shown in the tables below.

Table 5.11: Real world recovery creation results.

Test	Processing Time (ms)	Dubins Length (m)	Hybrid A* length (m)
1	150.99	5.13	3.42
2	121.42	3.90	2.60
3	238.17	6.34	5.19
4	254.42	3.92	6.35
5	242.21	2.53	5.93
Mean	201.44	4.36	4.70
Standard Deviation	60.76	1.44	1.62

Table 5.12: Real world recovery tracking results.

Test	Time to goal (s)	Total Length (m)
1	56.23	8.54
2	24.35	6.50
3	32.87	11.53
4	not reached	10.27
5	not reached	8.46
Mean	N/A	9.06
Standard Deviation	N/A	1.92

As shown in the previous tables, there were two tests with very similar initial and goal positions, the robot was not able to reach the goal pose. Since the robot would constantly try to replan its path, a "not reached" classification would be applied if the robot could not reach the goal in two minutes.



Figure 5.7: Test where the resulting path was slightly different from the originally planned one.



Figure 5.8: Test where the path had too many manoeuvres for the controller to handle.



Figure 5.9: Recovery correction of the previous test setup in the real world environment.

5.2 Obstacle detection Tests

The obstacle detection tests were also conducted in the simulated environment and the real world, however, instead of running it in the corridor, it was run in the concealed room as it had more obstacles and possibility of dynamic obstacles.

5.2.1 Simulation Results

The simulation tests were conducted by moving an obstacle in the gazebo environment and checking if the robot was able to detect it and stop before colliding with it. This was achieved by giving the robot an achievable goal pose and moving the obstacle in front while the robot is following the path.

For this test the parameterised range was one meter.

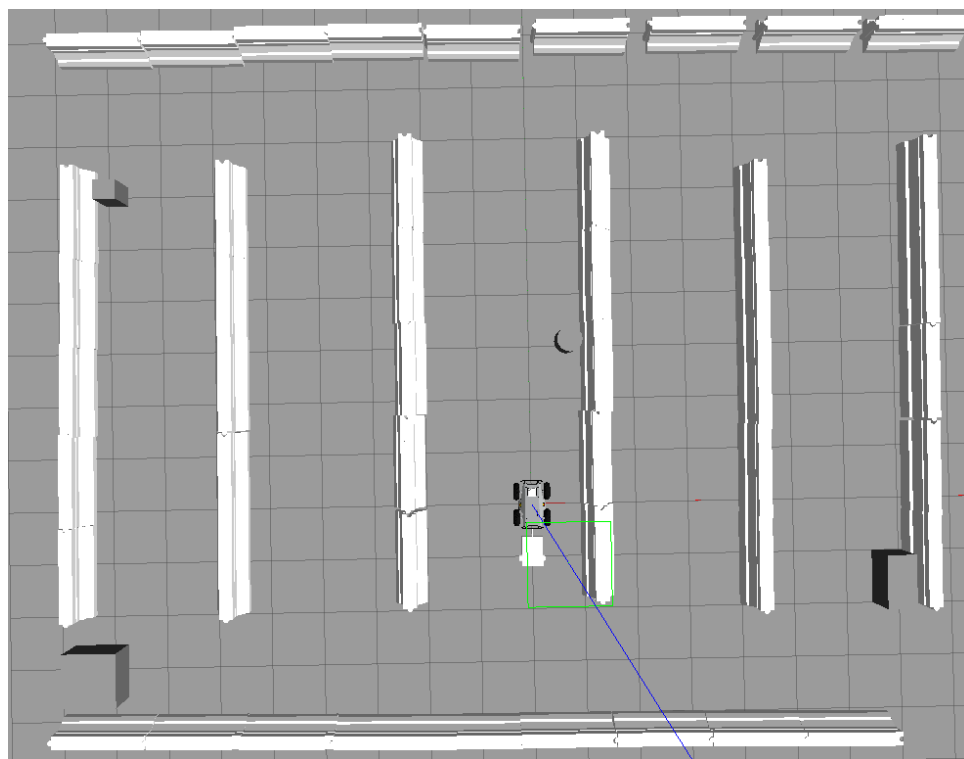


Figure 5.10: Initial configuration in the simulated environment.

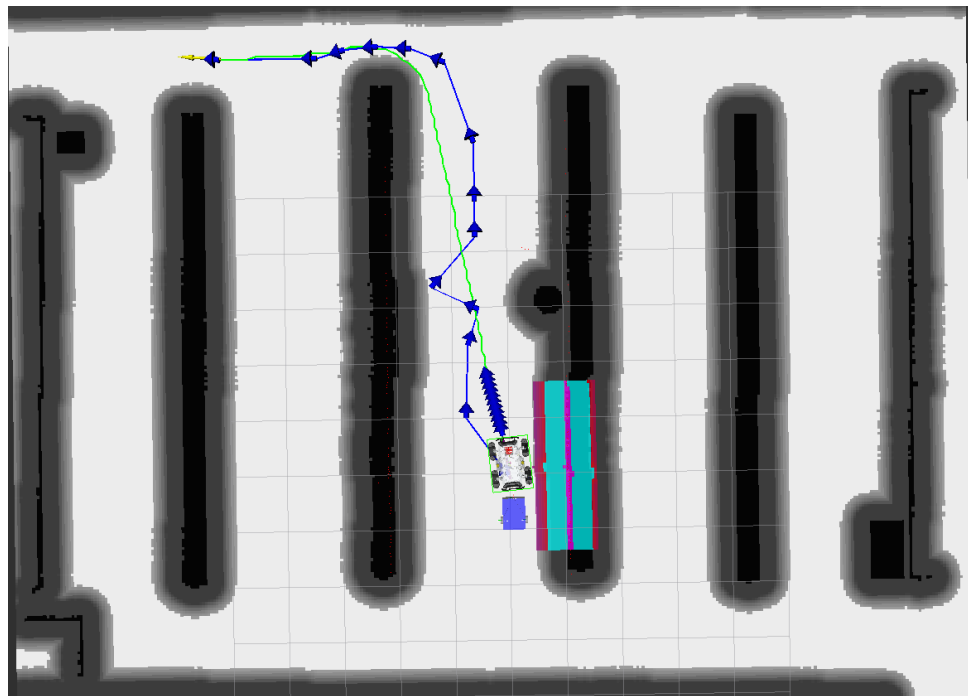


Figure 5.11: Initial path in the simulated environment. The blue arrows coming out from the tractor represent the collision detection range.

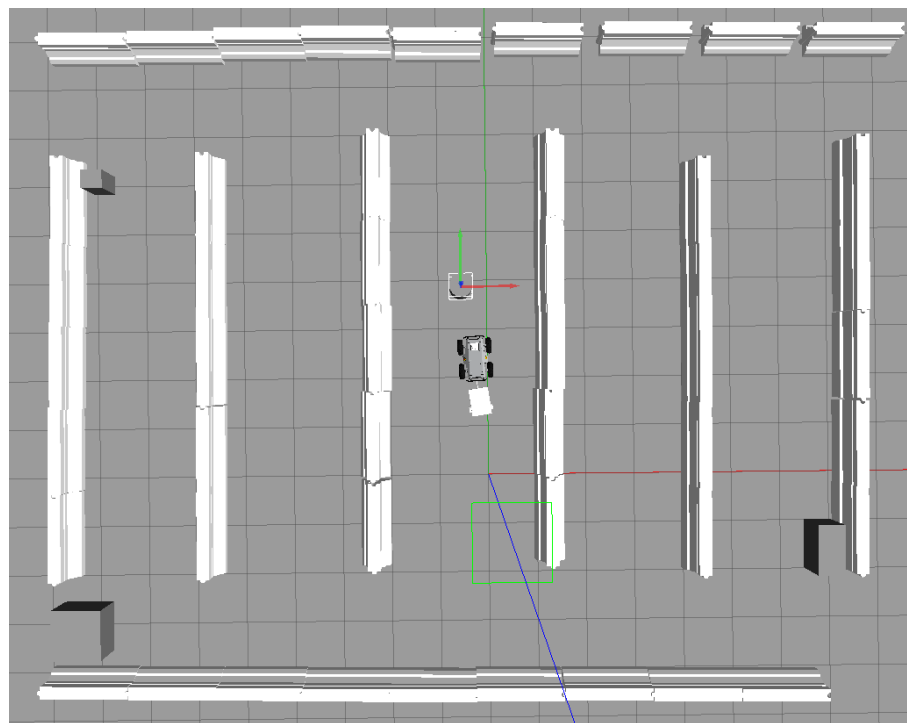


Figure 5.12: Final configuration in the simulated environment. The cylinder was moved and the robot stopped in the parameterised range.

As observed in figure 5.13, the robot was able to detect the obstacle and come to a stop before colliding with it. The same test was done with a reversing manoeuvre, and both can be seen in an annexed video.

5.2.2 Real World Results

The real world tests results can be shown in an annexed video, however, the results were very similar and the robot was able to come to a stop and resume its path after the obstacle was removed. There was no test for the reversing manoeuvre due to the lack of a physical trailer, which would be the one to collide with any obstacle in such a scenario.

5.3 Discussion

In this section, there will be an overview of the obtained results as well as some insights into the performance of the proposed methods as well as their viability.

5.3.1 Path Tracking

When it came to path tracking, if the goal pose was reachable by only moving in the forwards direction, the robot would have absolutely no problem reaching it, even with the presence of obstacles. However, when the goal pose required a change in direction or a hitching manoeuvre, depending on the current configuration of the robot and the environment, it couldn't be assured that the robot would be able to reach it. This, of course, is due to the fact that the trailer's controller, despite being designed to account for such scenarios, struggled when multiple manoeuvres were required in quick succession, leading the robot to positions which weren't initially in the path and could only be recovered with a new planning iteration, like in ???. This fact doesn't invalidate the proposed solution as it still provides a successful navigation experience in the majority of scenarios and only fails in specific situations where the robot is in very narrow spaces and is required to reverse or in position where the density of voronoi nodes is too low to provide a path which avoids the obstacles.

Addressing now the collected data on the tests, a relation of the processing time and the length of the path and the length of the recovery segment could be observed. It was found that as the length of the path increased, the processing time also increased, which is expected as more computations are required to plan and execute longer paths. Also, the processing time required for recovery segments was higher than for the dubins segments, meaning that paths with similar lengths but one with half the length being Dubins and the other being the hybrid A* would have a higher processing time than the one with just the Dubins segments. This is also to be expected as the hybrid A* launches additional nodes during the search which increases the overall computational load, compared to the Dubins segment which simply calculates the mathematical path using a closed-form solution.

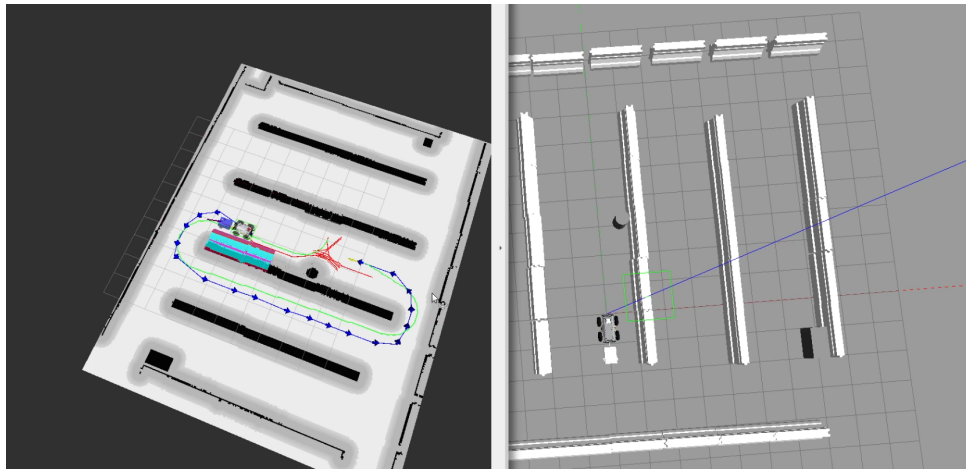


Figure 5.13: Failed attempt where the robot needed to invert its pose within the corridor, leading to multiple successive changes in directions. Video also annexed.

Table 5.13: Mean processing time and lengths of the paths in the simulation tests conducted.

Test	Mean Processing Time (ms)	Mean Total Length (m)
Direct Path	15.91	5.23
Obstructed Path	18.77	11.38
Recovery Test	24.21	10.62

Table 5.14: Mean processing time and lengths of the paths in the real world tests conducted.

Test	Mean Processing Time (ms)	Mean Total Length (m)
Direct Path	59.14	8.87
Obstructed Path	60.59	11.89
Recovery Test	201.44	9.06

Table 5.15: Standard deviation processing time and lengths of the paths in the simulation tests conducted.

Test	SD Processing Time (ms)	SD Total Length (m)
Direct Path	0.69	0.00
Obstructed Path	1.19	0.00
Recovery Test	1.47	0.00

Table 5.16: Standard deviation from processing time and lengths of the paths in the real world tests conducted.

Test	SD Processing Time (ms)	SD Total Length (m)
Direct Path	6.27	0.02
Obstructed Path	5.11	0.02
Recovery Test	60.76	1.92

From the collected data, it is possible to assert that the previously mentioned trends hold true, both in the simulations as in the real world tests. It was also observed that the recovery process was significantly more computationally complex than the Dubins segments, specially in the real world tests, where the processing power is significantly lower than in the simulation environment. Despite this, the time required to calculate a path proved to be fast enough for the allocated task, as it would not be a critical issue in overall performance. Despite this, the processing time would still be a factor to consider in future optimizations.

5.3.2 Obstacle Detection and Safety

The obstacle detection module worked perfectly fine, both in simulation and in the real world, with the only aspect to be improved being the time to detect and add the obstacles to the local costmap. However, this improvement is outside the scope of this work as it is a standard tool provided by the [NAV2](#) stack.

CONCLUSION AND FUTURE WORK

6.1 Conclusion

This thesis presented the development, implementation, and validation of an autonomous navigation system for a tractor-trailer system to be used for pesticide spraying in agricultural environments. The work began by identifying the pressing need for increased efficiency and safety in agriculture, especially in the context of global food demand and the challenges posed by traditional farming methods. The proposed solution was designed to address the unique difficulties of tractor-trailer navigation, including non-holonomic constraints, modularity, and the need for collision safety in complex and constrained spaces.

The literature review established the context for mobile robotics in smart agriculture, motion planning approaches, and control methods, highlighting the importance of the design of an efficient navigation system. The architecture chapter detailed the design, hardware selection, and system overview. The implementation chapter described the use of the [ROS2](#) framework and [NAV2](#) stack, which enabled modular development, and seamless integration of hardware and software components. The planning algorithm, combining Voronoi Hybrid A* and Dubins paths, provided feasible path generation, while the controller ensured accurate path tracking in the majority of scenarios.

Testing in both simulated and real-world environments demonstrated the system's reliability, safety, and practical viability. The results showed that the robot could successfully navigate direct, obstructed, and most recovery paths, as well as avoid and detect collisions.

Overall, the thesis achieved its objectives and contributed a solid foundation for autonomous agricultural robotics. The successful implementation and validation of the proposed system demonstrates its potential for real-world deployment, offering significant development in the study of solutions for the tractor-trailer system. The work also provides valuable insights and methodologies that can be extended to other agricultural and industrial applications.

6.2 Future Work

While the current system proved successful, there are several promising directions for future research and development. Integrating GPS-based localization would greatly enhance the robot's performance in large-scale agricultural fields, where map-based localization may be limited. This improvement would allow for more accurate global positioning and facilitate operations over extended areas, making the system even more versatile and scalable.

Another important avenue is the redesign of the controller. The controller used in this work, while effective in many scenarios, demonstrated difficulty when navigating in consecutive changes in direction and curved manoeuvres. By exploring more advanced control strategies such as [MPC](#) or machine learning approaches, the system could achieve more precise control over its movements, leading to smoother and more reliable navigation.

In summary, this thesis lays a foundation for autonomous agricultural robotics. The successful implementation and validation of the proposed system demonstrate its real-world potential, and the suggested future improvements offer exciting opportunities for further research and innovation in the field.

BIBLIOGRAPHY

- [1] J. M. Lourenço. *The NOVAtesis L^AT_EX Template User's Manual*. NOVA University Lisbon. 2021. URL: <https://github.com/joaomlourenco/novathesis/raw/main/template.pdf> (cit. on p. i).
- [2] A. Hafeez et al. "Implementation of drone technology for farm monitoring & pesticide spraying: A review". In: *Information Processing in Agriculture* 10.2 (2023), pp. 192–203. ISSN: 2214-3173. doi: <https://doi.org/10.1016/j.inpa.2022.02.002> (cit. on p. 1).
- [3] S. Qazi, B. A. Khawaja, and Q. U. Farooq. "IoT-Equipped and AI-Enabled Next Generation Smart Agriculture: A Critical Review, Current Challenges and Future Trends". In: *IEEE Access* 10 (2022), pp. 21219–21235. doi: [10.1109/ACCESS.2022.3152544](https://doi.org/10.1109/ACCESS.2022.3152544) (cit. on p. 3).
- [4] L. F. P. Oliveira, A. P. Moreira, and M. F. Silva. "Advances in Agriculture Robotics: A State-of-the-Art Review and Challenges Ahead". In: *Robotics* 10.2 (2021). ISSN: 2218-6581. doi: [10.3390/robotics10020052](https://doi.org/10.3390/robotics10020052). URL: <https://www.mdpi.com/2218-6581/10/2/52> (cit. on p. 3).
- [5] D. F. Yépez Ponce et al. "Mobile robotics in smart farming: current trends and applications". In: *Frontiers in Artificial Intelligence* 6 (2023-08). doi: [10.3389/frai.2023.1213330](https://doi.org/10.3389/frai.2023.1213330) (cit. on pp. 3, 4).
- [6] V. Moysiadis et al. "Mobile Robotics in Agricultural Operations: A Narrative Review on Planning Aspects". In: *Applied Sciences* 10.10 (2020). ISSN: 2076-3417. doi: [10.3390/app10103453](https://doi.org/10.3390/app10103453). URL: <https://www.mdpi.com/2076-3417/10/10/3453> (cit. on p. 4).
- [7] K. G. Fue et al. "An Extensive Review of Mobile Agricultural Robotics for Field Operations: Focus on Cotton Harvesting". In: *AgriEngineering* 2.1 (2020), pp. 150–174. ISSN: 2624-7402. doi: [10.3390/agriengineering2010010](https://doi.org/10.3390/agriengineering2010010). URL: <https://www.mdpi.com/2624-7402/2/1/10> (cit. on p. 4).

- [8] L.-B. Chen, X.-R. Huang, and W.-H. Chen. "Design and Implementation of an Artificial Intelligence of Things-Based Autonomous Mobile Robot System for Pitaya Harvesting". In: *IEEE Sensors Journal* 23.12 (2023), pp. 13220–13235. doi: [10.1109/JSEN.2023.3270844](https://doi.org/10.1109/JSEN.2023.3270844) (cit. on p. 4).
- [9] E.-T. Baek and D.-Y. Im. "ROS-Based Unmanned Mobile Robot Platform for Agriculture". In: *Applied Sciences* 12.9 (2022). issn: 2076-3417. doi: [10.3390/app12094335](https://doi.org/10.3390/app12094335). URL: <https://www.mdpi.com/2076-3417/12/9/4335> (cit. on p. 4).
- [10] M. G. Tamizi, M. Yaghoubi, and H. Najjaran. "A review of recent trend in motion planning of industrial robots". In: *International Journal of Intelligent Robotics and Applications* 7.2 (2023), pp. 253–274. doi: <https://doi.org/10.1007/s10845-021-01867-z> (cit. on p. 5).
- [11] L. Liu et al. "Path planning techniques for mobile robots: Review and prospect". In: *Expert Systems with Applications* 227 (2023), p. 120254. issn: 0957-4174. doi: <https://doi.org/10.1016/j.eswa.2023.120254>. URL: <https://www.sciencedirect.com/science/article/pii/S095741742300756X> (cit. on p. 5).
- [12] B. Patle et al. "A review: On path planning strategies for navigation of mobile robot". In: *Defence Technology* 15.4 (2019), pp. 582–606. issn: 2214-9147. doi: <https://doi.org/10.1016/j.dt.2019.04.011>. URL: <https://www.sciencedirect.com/science/article/pii/S2214914718305130> (cit. on p. 6).
- [13] S. Xie et al. "Distributed Motion Planning for Safe Autonomous Vehicle Overtaking via Artificial Potential Field". In: *IEEE Transactions on Intelligent Transportation Systems* 23.11 (2022), pp. 21531–21547. doi: [10.1109/TITS.2022.3189741](https://doi.org/10.1109/TITS.2022.3189741) (cit. on p. 9).
- [14] C. Warren. "Global path planning using artificial potential fields". In: (1989), 316–321 vol.1. doi: [10.1109/ROBOT.1989.100007](https://doi.org/10.1109/ROBOT.1989.100007) (cit. on p. 9).
- [15] Y. Li et al. "Path planning of robot based on artificial potential field method". In: 6 (2022), pp. 91–94. doi: [10.1109/ITOEC53115.2022.9734712](https://doi.org/10.1109/ITOEC53115.2022.9734712) (cit. on p. 9).
- [16] W. Xinyu et al. "Bidirectional Potential Guided RRT* for Motion Planning". In: *IEEE Access* 7 (2019), pp. 95046–95057. doi: [10.1109/ACCESS.2019.2928846](https://doi.org/10.1109/ACCESS.2019.2928846) (cit. on p. 9).
- [17] A. A. Ravankar et al. "HPPRM: Hybrid Potential Based Probabilistic Roadmap Algorithm for Improved Dynamic Path Planning of Mobile Robots". In: *IEEE Access* 8 (2020), pp. 221743–221766. doi: [10.1109/ACCESS.2020.3043333](https://doi.org/10.1109/ACCESS.2020.3043333) (cit. on p. 10).
- [18] J. Wang et al. "Efficient Robot Motion Planning Using Bidirectional-Unidirectional RRT Extend Function". In: *IEEE Transactions on Automation Science and Engineering* 19.3 (2022), pp. 1859–1868. doi: [10.1109/TASE.2021.3130372](https://doi.org/10.1109/TASE.2021.3130372) (cit. on p. 11).
- [19] H.-y. Zhang, W.-m. Lin, and A.-x. Chen. "Path Planning for the Mobile Robot: A Review". In: *Symmetry* 10.10 (2018). issn: 2073-8994. doi: [10.3390/sym10100450](https://doi.org/10.3390/sym10100450). URL: <https://www.mdpi.com/2073-8994/10/10/450> (cit. on p. 11).

BIBLIOGRAPHY

- [20] L. Blasi et al. "Path Planning and Real-Time Collision Avoidance Based on the Essential Visibility Graph". In: *Applied Sciences* 10.16 (2020). issn: 2076-3417. doi: [10.3390/app10165613](https://doi.org/10.3390/app10165613). URL: <https://www.mdpi.com/2076-3417/10/16/5613> (cit. on p. 11).
- [21] L. E. Dubins. "On Curves of Minimal Length with a Constraint on Average Curvature, and with Prescribed Initial and Terminal Positions and Tangents". In: *American Journal of Mathematics* 79.3 (1957), pp. 497–516. issn: 00029327, 10806377. doi: <https://doi.org/10.2307/2372560>. URL: <http://www.jstor.org/stable/2372560> (visited on 2024-09-28) (cit. on p. 11).
- [22] W. Lee, G.-H. Choi, and T.-w. Kim. "Visibility graph-based path-planning algorithm with quadtree representation". In: *Applied Ocean Research* 117 (2021), p. 102887. issn: 0141-1187. doi: <https://doi.org/10.1016/j.apor.2021.102887>. URL: <https://www.sciencedirect.com/science/article/pii/S0141118721003588> (cit. on p. 11).
- [23] J. Wang and M. Q.-H. Meng. "Optimal Path Planning Using Generalized Voronoi Graph and Multiple Potential Functions". In: *IEEE Transactions on Industrial Electronics* 67.12 (2020), pp. 10621–10630. doi: [10.1109/TIE.2019.2962425](https://doi.org/10.1109/TIE.2019.2962425) (cit. on p. 12).
- [24] S. Poudel, M. Y. Arafat, and S. Moh. "Bio-Inspired Optimization-Based Path Planning Algorithms in Unmanned Aerial Vehicles: A Survey". In: *Sensors* 23.6 (2023). issn: 1424-8220. doi: [10.3390/s23063051](https://doi.org/10.3390/s23063051). URL: <https://www.mdpi.com/1424-8220/23/6/3051> (cit. on p. 13).
- [25] M. Saska et al. "Robot Path Planning using Particle Swarm Optimization of Ferguson Splines". In: *2006 IEEE Conference on Emerging Technologies and Factory Automation*. 2006, pp. 833–839. doi: [10.1109/ETFA.2006.355416](https://doi.org/10.1109/ETFA.2006.355416) (cit. on p. 13).
- [26] Q. Luo et al. "Research on path planning of mobile robot based on improved ant colony algorithm". In: *Neural Computing and Applications* 32 (2020), pp. 1555–1566. doi: <https://doi.org/10.1007/s00521-019-04172-2> (cit. on p. 14).
- [27] X. Dai et al. "Mobile robot path planning based on ant colony algorithm with A* heuristic method". In: *Frontiers in neurorobotics* 13 (2019), p. 15. doi: [10.3389/fnbot.2019.00015](https://doi.org/10.3389/fnbot.2019.00015) (cit. on p. 14).
- [28] X. Xie, Z. Tang, and J. Cai. "The multi-objective inspection path-planning in radioactive environment based on an improved ant colony optimization algorithm". In: *Progress in Nuclear Energy* 144 (2022), p. 104076. issn: 0149-1970. doi: <https://doi.org/10.1016/j.pnucene.2021.104076>. URL: <https://www.sciencedirect.com/science/article/pii/S0149197021004303> (cit. on p. 14).

- [29] H. Guo et al. "Optimal search path planning for unmanned surface vehicle based on an improved genetic algorithm". In: *Computers & Electrical Engineering* 79 (2019), p. 106467. doi: <https://doi.org/10.1016/j.compeleceng.2019.106467> (cit. on p. 15).
- [30] C. E. Okereke et al. "An Overview of Machine Learning Techniques in Local Path Planning for Autonomous Underwater Vehicles". In: *IEEE Access* 11 (2023), pp. 24894–24907. doi: [10.1109/ACCESS.2023.3249966](https://doi.org/10.1109/ACCESS.2023.3249966) (cit. on p. 15).
- [31] S. Aggarwal and N. Kumar. "Path planning techniques for unmanned aerial vehicles: A review, solutions, and challenges". In: *Computer Communications* 149 (2020), pp. 270–299. issn: 0140-3664. doi: <https://doi.org/10.1016/j.comcom.2019.10.014> (cit. on p. 15).
- [32] S. Aradi. "Survey of Deep Reinforcement Learning for Motion Planning of Autonomous Vehicles". In: *IEEE Transactions on Intelligent Transportation Systems* 23.2 (2022), pp. 740–759. doi: [10.1109/TITS.2020.3024655](https://doi.org/10.1109/TITS.2020.3024655) (cit. on p. 16).
- [33] S. Sombolestan, A. Rasooli, and S. Khodaygan. "Optimal path-planning for mobile robots to find a hidden target in an unknown environment based on machine learning". In: *Journal of ambient intelligence and humanized computing* 10 (2019), pp. 1841–1850. doi: <https://doi.org/10.1007/s12652-018-0777-4> (cit. on p. 16).
- [34] J. Wang et al. "Neural RRT*: Learning-Based Optimal Path Planning". In: *IEEE Transactions on Automation Science and Engineering* 17.4 (2020), pp. 1748–1758. doi: [10.1109/TASE.2020.2976560](https://doi.org/10.1109/TASE.2020.2976560) (cit. on p. 16).
- [35] S. Macenski et al. "Regulated pure pursuit for robot path tracking". In: *Autonomous Robots* 47.6 (2023), pp. 685–694. doi: <https://doi.org/10.1007/s10514-023-10097-6> (cit. on p. 16).
- [36] E. Kayacan and G. Chowdhary. "Tracking error learning control for precise mobile robot path tracking in outdoor environment". In: *Journal of Intelligent & Robotic Systems* 95 (2019), pp. 975–986. doi: <https://doi.org/10.1007/s10846-018-0916-3> (cit. on p. 17).
- [37] M. Kobayashi and N. Motoi. "Local Path Planning: Dynamic Window Approach With Virtual Manipulators Considering Dynamic Obstacles". In: *IEEE Access* 10 (2022), pp. 17018–17029. doi: [10.1109/ACCESS.2022.3150036](https://doi.org/10.1109/ACCESS.2022.3150036) (cit. on p. 17).
- [38] I. Ullah et al. "Mobile robot localization: Current challenges and future prospective". In: *Computer Science Review* 53 (2024), p. 100651. issn: 1574-0137. doi: <https://doi.org/10.1016/j.cosrev.2024.100651>. url: <https://www.sciencedirect.com/science/article/pii/S1574013724000352> (cit. on p. 18).
- [39] K. S. Chong and L. Kleeman. "Accurate odometry and error modelling for a mobile robot". In: *Proceedings of International Conference on Robotics and Automation*. Vol. 4. 1997, 2783–2788 vol.4. doi: [10.1109/ROBOT.1997.606708](https://doi.org/10.1109/ROBOT.1997.606708) (cit. on p. 18).

BIBLIOGRAPHY

- [40] M.-A. Chung and C.-W. Lin. "An Improved Localization of Mobile Robotic System Based on AMCL Algorithm". In: *IEEE Sensors Journal* 22.1 (2022), pp. 900–908. doi: [10.1109/JSEN.2021.3126605](https://doi.org/10.1109/JSEN.2021.3126605) (cit. on p. 18).
- [41] Y. K. Tee and Y. C. Han. "Lidar-Based 2D SLAM for Mobile Robot in an Indoor Environment: A Review". In: *2021 International Conference on Green Energy, Computing and Sustainable Technology (GECOST)*. 2021. doi: [10.1109/GECOST52368.2021.9538731](https://doi.org/10.1109/GECOST52368.2021.9538731) (cit. on p. 18).
- [42] A. Tourani et al. "Visual SLAM: What Are the Current Trends and What to Expect?" In: *Sensors* 22.23 (2022). issn: 1424-8220. doi: [10.3390/s22239297](https://doi.org/10.3390/s22239297) (cit. on p. 18).
- [43] T. Thakkar and A. Sinha. "Motion Planning for Tractor-Trailer System". In: *2021 Seventh Indian Control Conference (ICC)*. 2021, pp. 93–98. doi: [10.1109/ICC54714.2021.9703119](https://doi.org/10.1109/ICC54714.2021.9703119) (cit. on pp. 18, 19, 22).
- [44] Z. Wang et al. "Motion Planning and Model Predictive Control for Automated Tractor-Trailer Hitching Maneuver". In: *2022 IEEE Conference on Control Technology and Applications (CCTA)*. 2022, pp. 676–682. doi: [10.1109/CCTA49430.2022.9966181](https://doi.org/10.1109/CCTA49430.2022.9966181) (cit. on p. 18).
- [45] N. Ito et al. "Configuration-aware Model Predictive Motion Planning in Narrow Environment for Autonomous Tractor-trailer Mobile Robot". In: *IECON 2021 – 47th Annual Conference of the IEEE Industrial Electronics Society*. 2021, pp. 1–7. doi: [10.1109/IECON48115.2021.9589596](https://doi.org/10.1109/IECON48115.2021.9589596) (cit. on pp. 19, 22).
- [46] P. Svestka and J. Vleugels. "Exact motion planning for tractor-trailer robots". In: *Proceedings of 1995 IEEE International Conference on Robotics and Automation*. Vol. 3. 1995, 2445–2450 vol.3. doi: [10.1109/ROBOT.1995.525626](https://doi.org/10.1109/ROBOT.1995.525626) (cit. on pp. 20, 22).
- [47] N. T. Hoang et al. "Artificial potential field based motion planning for autonomous tractor-trailer vehicles". In: *Results in Engineering* 27 (2025), p. 105936. issn: 2590-1230. doi: <https://doi.org/10.1016/j.rineng.2025.105936> (cit. on pp. 21, 22).
- [48] R. Oliveira et al. "Optimization-Based On-Road Path Planning for Articulated Vehicles This work was partially supported by the Wallenberg AI, Autonomous Systems and Software Program (WASP) funded by the Knut and Alice Wallenberg Foundation." In: *IFAC-PapersOnLine* 53.2 (2020). 21st IFAC World Congress, pp. 15572–15579. issn: 2405-8963. doi: <https://doi.org/10.1016/j.ifacol.2020.12.2402> (cit. on pp. 21, 22).
- [49] *Nav2 documentation*. <https://docs.nav2.org/>. Accessed: 2025-08-07 (cit. on p. 33).
- [50] *Agilex Scout dimensions*. <https://static.generation-robots.com/media/datasheet-agilex-robotics-scout2.0-en.pdf>. Accessed: 2025-07-29 (cit. on p. 35).

- [51] *Scout ROS2 repository*. https://github.com/agilexrobotics/scout_ros2/tree/main. Accessed: 2025-08-08 (cit. on p. 38).
- [52] *RoboSense LiDAR SDK*. https://github.com/RoboSense-LiDAR/rslidar_sdk. Accessed: 2025-08-08 (cit. on p. 38).
- [53] *VoronoiScipy*. <https://docs.scipy.org/doc/scipy/reference/generated/scipy.spatial.Voronoi.html>. Accessed: 2025-08-07 (cit. on p. 40).

I

ANNEX 1 CLIPS

Here are the urls for the recordings of the various tests:

[Straight Tests](#)

[Curved Tests](#)

[Recovery Tests](#)

[Failed Attempts](#)

Here are the urls for the recordings of the obstacle detection test:

[Obstacle Detection Tests](#)

II

ANNEX 2 CODE

Here is the github repository with the code used in in this thesis. The repository is a fork from a privous student Rafael Carvalho and includes various packages for additional robots. The packages that were relevant and developed in this thesis are the following:

- `scout_description`, for the URDF and trailer publisher
- `pp_controller`, for the controller and obstacle detection
- `astar_planner`, for the path planning algorithm

https://github.com/TomasPedreira/tese_ws





2025 MOTION PLANNING FOR A TRACTOR-TRAILER SYSTEM IN SMART AGRICULTURE